Synthesis and Structural Characterization of Lanthanide(III) Texaphyrins

Jonathan L. Sessler,* Tarak D. Mody, Gregory W. Hemmi, and Vincent Lynch

Department of Chemistry and Biochemistry, University of Texas at Austin, Austin, Texas 78712

Received January 7, 1993

The synthesis and characterization of several lanthanide(III) texaphyrin complexes of 4,5,9,24-tetraethyl-16,17-dimethoxy-10,23-dimethyl-13,20,25,26,27-pentaazapentacyclo[20.2.1.1^{3,6}.1^{8,11}.0^{14,19}]heptacosa-1,3,5,7,9,11(27),-12,14,16,18,20,22(25),23-tridecaene (**2**), 4,5,9,24-tetraethyl-16,17-bis((3-hydroxypropyl)oxy)-10,23-dimethyl-13,20,25,26,27-pentaazapentacyclo-[20.2.1.1^{3,6}.1^{8,11}.0^{14,19}]heptacosa-1,3,5,7,9,11(27),12,14(19),15,17,20,22(25),-23-tridecaene (**21**), and 4,5-diethyl-10,23-dimethyl-9,24-bis(3-hydroxypropyl)-16,17-(3-hydroxypropyloxy)-13,-20,25,26,27-pentaazapentacyclo[20.2.1.1^{3,6}.1^{8,11}.0^{14,19}]heptacosa-1,3,5,7,9,11(27),12,14,16,18,20,22(25),23-tridecaene (**30**), respectively, are reported. Single crystals suitable for X-ray diffraction were obtained for the La(III) complex **3**, the Gd(III) complexes **9** and **37**, the Eu(III) complex **36**, and the Lu(III) complex **22**, by dissolving the respective complex in MeOH/$CHCl_3$ and layering with diethyl ether. The five lanthanide(III) texaphyrin complexes all crystallize in the triclinic space group, $P\bar{1}$ (No. 2), with $Z = 2$. The final R's, for data collected at reduced temperatures (≤−90 °C), were 0.0412 for **3**, 0.0373 for **9**, 0.0293 for **22**, 0.0320 for **36**, and 0.0477 for **37**. The complexes are characterized by five-coordination from the texaphyrin, a coordinated methanol molecule on one side and at least one symmetrically bidentate NO_3^- ion opposite the methanol. The 10-coordinate La(III) complex **3** has two bidentate NO_3^- ions on the same side of the macrocycle. The europium(III) and gadolinium(III) texaphyrins **36** and **37** are structurally isomorphous and are 9-coordinate species with a bidentate NO_3^- ion and a methanol molecule on the top side of the macrocycle. On the other hand, the lutetium(III) texaphyrin is 8-coordinate with only a single bidentate NO_3^- ion chelated to the "top" side of complex. In an unusual case of disorder, the gadolinium-(III) texaphyrin **9** has both 9- and 10-coordinate species present in the solid state. The geometry of the 9-coordinate species is much like that found in **36** and **37**, while the 10-coordinate Gd(III) species is similar to the La(III) species **3**. Together, these structures reflect both the decrease in coordination number and the intrinsic contraction in cation size observed as the lanthanide series is transversed. For instance, an average decrease in nitrogen-to-metal bond length of 0.12 Å is found when comparing the 10-coordinate La(III) complex **3** to the 9-coordinate gadolinium(III) texaphyrin species **37** and a decrease of 0.075 Å is observed when comparing this latter Gd(III) complex to the 8-coordinate Lu(III) system **22**. Similarly, the 10-coordinate La(III) center in **3** is found to be 0.91 Å from the mean plane through the five nitrogen donors of the macrocycle while the 8-coordinate Lu(III) center in **22** is only 0.27 Å from the plane. Finally, the root-mean-square deviation from planarity for the atoms of the macrocycle core is 0.15 Å in **3** and only 0.072 Å in **22**, as compared to 0.097, 0.122, and 0.120 Å in **9**, **36**, and **37**, respectively.

Since the discovery of the lanthanide elements, the coordination chemistry of the trivalent lanthanide(III) ions has received considerable attention with the level of this attention increasing dramatically in recent years.[1] For instance, the interactions of the lanthanide ions with macrocyclic ligands, such as the crown ethers,[2,3] cryptands,[4] Schiff-base macrocycles,[5] and porphyrin derivatives,[6,7] to name a few, have been studied extensively over the last two decades. However, currently there are relatively few macrocyclic ligand systems that are capable of forming substitutionally inert complexes with these cations, especially in water. The design of ligands capable of forming stable lanthanide(III) complexes not only would allow further study of the coordination properties of the rare earth ions but also would enable chemists to exploit more fully certain now-appreciated properties of these cations. For example, Ln(III) complexes have found uses as NMR shift reagents,[8] as luminescent probes for complex

(1) (a) Moeller, T. *The Chemistry of the Lanthanides*; Reinhold: New York, 1963; Chapter 1. (b) Choppin, G. R. In *Lanthanide Probes in Life, Chemical and Earth Sciences: Theory and Practice*; Bunzli, J.-C. G., Choppin, G. R., Eds.; Elsevier: Amsterdam, 1989; Chapter 1.

(2) For some leading references of lanthanide chemistry with crown ethers, see: (a) Pedersen, C. J. *J. Am. Chem. Soc.* **1969**, *89*, 2495–2496. (b) Pedersen, C. J. *J. Am. Chem. Soc.* **1969**, *89*, 7017–7036. (c) Cassol, A.; Seminaro, A.; De Paoli, G. *Inorg. Nucl. Chem. Lett.* **1973**, *9*, 1163–1168. (d) Bunzli, J.-C. G.; Wessner, D. *Helv. Chim. Acta* **1978**, *61*, 1454–1461. (e) Bunzli, J.-C. G.; Wessner, D.; Oanh, H. T. T. *Inorg. Chim Acta* **1979**, *32*, L33–L36. (f) Tongbu, L.; Xinmin, G.; Ning, T.; Minyu, T. *Polyhedron* **1990**, *9*, 2371–2374. (g) Harman, M. E.; Hart, F. A.; Hursthouse, M. B.; Moss, G. P.; Raithby, P. R. *J. Chem. Soc., Chem. Commun.* **1976**, 396–397. (h) Chen, Z.; Dettman, H.; Detellier, C. *Polyhedron* **1989**, *8*, 2029–2033. (i) Bunzli, J.-C. G.; Pilloud, F. *Inorg. Chem.* **1989**, *28*, 2638–2642. (j) Cassol, A.; Di Bernardo, P.; Zanonato, P. L.; Tolazzi, M.; Tomat, G. *Inorg. Chim. Acta* **1990**, *171*, 217–221 and references therein.

(3) For leading references of lanthanide chemistry with azacrown ethers, see: (a) Loncin, M. F.; Desreux, J. F.; Merciny, E. *Inorg. Chem.* **1986**, *25*, 2646–2648. (b) Sherry, A. D.; Brown, R. D., III; Geraldes, C. F. G. C.; Koenig, S. H.; Kuan, K.-T.; Spiller, M. *Inorg. Chem.* **1989**, *28*, 620–622. (c) Brucher, E.; Cortes, S.; Chavez, F.; Sherry, A. D. *Inorg. Chem.* **1991**, *30*, 2092–2097. (d) Prasad, J. S.; Okuniewicz, F. J.; Delaney, E. J.; Dischino, D. D. *J. Chem. Soc., Perkin Trans. 1* **1991**, 3329–3332. (e) Dischino, D. D.; Delaney, E. J.; Emswiler, J. E.; Gaughan, G. T.; Prasad, J. S.; Srivastava, S. K.; Tweedle, M. F. *Inorg. Chem.* **1991**, *30*, 1265–1269. (f) Kodama, M.; Koike, T.; Mahatma, A. B.; Kimura, E. *Inorg. Chem.* **1991**, *30*, 1270–1273. (g) Aime, S.; Botta, M.; Ermondi, G.; Fedeli, F.; Uggeri, F. *Inorg. Chem.* **1992**, *31*, 1100–1103 and references therein. (h) Chang, C. A.; Sekhar, V. C. *Inorg. Chem.* **1987**, *26*, 1981–1985. (i) Chang, C. A.; Chang, P. H.-L.; Manchanda, V. K.; Kasprzyk, S. P. *Inorg. Chem.* **1988**, *27*, 3786–3789. (j) Chang, C. A.; Chang, P. H.-L.; Qin, S.-Y. *Inorg. Chem.* **1988**, *27*, 944–946. (k) Chen, D.; Squattrito, P. J.; Martell, A. E.; Clearfield, A. *Inorg. Chem.* **1990**, *29*, 4366–4368.

(4) For leading references on cryptands, see: (a) Dietrich, B.; Lehn, J. M.; Sauvage, J. P. *Tetrahedron Lett.* **1969**, *34*, 2885. (b) Torres, R. A.; Baisden, P. A. *Inorg. Chem.* **1989**, *28*, 2807–2810. (c) Gansow, O. A.; Kausar, A. R. *Inorg. Chim. Acta* **1983**, *72*, 39–41. (d) Gansow, O. A.; Kausar, A. R. *Inorg. Chim. Acta* **1985**, *95*, 1–6. (e) Hart, F. A.; Hursthouse, M. B.; Malik, K. M. A.; Moorhouse, S. *J. Chem. Soc., Chem. Commun.* **1978**, 549–550. (f) Ciampolini, M.; Dapporto, P.; Nardi, N. *J. Chem. Soc., Chem. Commun.* **1978**, 788–789. (g) Yee, E. L.; Gansow, O. A.; Weaver, M. J. *J. Am. Chem. Soc.* **1980**, *102*, 2278–2285. (h) Rebizant, J.; Spirlet, M. R.; Barthelemy, P. P.; Desreux, J. F. *J. Inclusion Phenom.* **1987**, *5*, 505–513. (i) Yang, G.; Liu, S.; Jin, Z. *Inorg. Chim. Acta* **1987**, *131*, 125–128. (j) Marolleau, I.; Gisselbrecht, J.-P.; Gross, M.; Arnaud-Neu, F.; Schwing-Weill, M.-J. *J. Chem. Soc., Dalton Trans.* **1990**, 1285–1290 and references therein. (k) Danil de Namor, A. F.; Ritt, M. C.; Schwing-Weill, M.-J.; Arnaud-Neu, F. *J. Chem. Soc., Faraday Trans.* **1990**, *86*, 89–93.

0020-1669/93/1332-3175$04.00/0

biomolecules,[9] and, more recently, as potential catalysts in the cleavage of RNA.[10]

Another important area of research associated with lanthanide coordination chemistry centers around the design of highly stable and kinetically inert complexes of gadolinium(III). Such complexes are of interest as possible paramagnetic imaging contrast agents for use in magnetic resonance imaging (MRI) applications.[11] The design of efficient gadolinium(III) imaging contrast agents is governed by stringent biological requirements such as high relaxivity, low *in vivo* toxicity, selective tissue localization, water solubility, rapid tissue clearance, and kinetic stability.[11]

Several approaches have been used to create stable (i.e. substitutionally inert) Gd(III) complexes in aqueous solution. A number of chelates have been designed which incorporate multiple carboxylate moieties in an effort to form complexes of high thermodynamic stability, such as diethylenetriaminepentaacetic acid (DTPA),[11-13] 1,4,7,10-tetraazacyclododecane-*N*,*N'*,*N''*,*N'''*-1,4,7,10-tetraacetic acid (DOTA), and 1,4,7,10-tetraazacyclododecane-*N*,*N'*,*N''*,*N'''*-1,4,7-triacetic acid (DO3A).[11,12,14] In fact, the bis(*N*-methylglucamine) salt of Gd^{III}DTPA (Magnevist),[12-13] bis(*N*-methylamide) of Gd^{III}DTPA (Omniscan),[13] and the 10-(2-hydroxypropyl) derivative of DO3A (Prohance)[14h-i] are currently being used clinically in certain enhanced tumor detection protocols. However, these types of imaging contrast agents suffer from low kinetic stability and possess low proton relaxivity. Therefore, there is interest in the development of new MRI contrast agents focusing on the design and synthesis of macrocyclic ligands capable of forming kinetically inert Gd(III) complexes.[11]

We have previously reported the preparation and general properties of a new class of "expanded porphyrins",[15] the so-called "texaphyrins".[16] During the course of this earlier work, we reported in preliminary fashion on the synthesis and initial characterization of a hydrolytically stable, all-alkyl-substituted

(5) For leading references to the macrocyclic Schiff-base lanthanide literature, see: (a) Fenton, D. E.; Vigato, P. A. *Chem. Soc. Rev.* **1988**, *17*, 69–90 and references therein. (b) Tsubomura, T.; Yasaku, K.; Sato, T.; Morita, M. *Inorg. Chem.* **1992**, *31*, 447–450. (c) Benetollo, F.; Bombieri, G.; De Cola, L.; Polo, A.; Smailes, D. L.; Vallarino, L. M. *Inorg. Chem.* **1989**, *28*, 3447–3452. (d) Smith, P. H.; Brainard, J. R.; Morris, D. E.; Jarvinen, G. D.; Ryan, R. R. *J. Am. Chem. Soc.* **1989**, *111*, 7437–7443. (e) Benetollo, F.; Polo, A.; Bombieri, G.; Fonda, K. K.; Vallarino, L. M. *Polyhedron* **1990**, *9*, 1411–1422. (f) Bombieri, G.; Benetollo, F.; Polo, A.; De Cola, L.; Hawkins, W. T.; Vallarino, L. M. *Polyhedron* **1989**, *8*, 2157–2167. (g) Kahwa, I. A.; Selbin, J.; O'Connor, C. J.; Foise, F. W.; McPherson, G. L. *Inorg. Chim. Acta* **1988**, *148*, 265–272. (h) Kahwa, I. A.; Fronczek, F. R.; Selbin, J. *Inorg. Chim. Acta* **1988**, *148*, 273–281. (i) Guerriero, P.; Casellato, U.; Tamburini, S.; Vigato, P. A.; Graziani, R. *Inorg. Chim. Acta* **1987**, *129*, 127–138. (j) Bunzli, J.-C. G.; Moret, E.; Casellato, U.; Guerriero, P.; Vigato, P. A. *Inorg. Chim. Acta* **1988**, *150*, 133–139. (k) Bullita, E.; Guerriero, P.; Tamburini, S.; Vigato, P. A. *J. Less-Common Met.* **1989**, *153*, 211–218. (l) Guerriero, P.; Vigato, P. A.; Bunzli, J.-C. G.; Moret, E. *J. Chem. Soc., Dalton Trans.* **1990**, 647–655. (m) Fenton, D. E.; Kitchen, S. J.; Spencer, C. M.; Tamburini, S.; Vigato, P. A. *J. Chem. Soc., Dalton Trans.* **1988**, 685–690. (n) Vigato, P. A.; Fenton, D. E. *Inorg. Chim. Acta* **1987**, *139*, 39–48.

(6) For leading references of lanthanide porphyrin chemistry, see: (a) Wong, C.-P.; Venteicher, R. F.; Horrocks, W. D., Jr. *J. Am. Chem. Soc.* **1974**, *96*, 7149–7150. (b) Buchler, J. W.; De Cian, A.; Fischer, J.; Kihn-Botulinski, M.; Paulus, H.; Weiss, R. *J. Am. Chem. Soc.* **1986**, *108*, 3652–3659. (c) Buchler, J. W.; Scharbert, B. *J. Am. Chem. Soc.* **1988**, *110*, 4272–4276. (d) Buchler, J. W.; De Cian, A.; Fischer, J.; Kihn-Botulinski, M.; Weiss, R. *Inorg. Chem.* **1988**, *27*, 339–345. (e) Buchler, J. W.; Kihn-Botulinski, M.; Loffler, J.; Wicholas, M. *Inorg. Chem.* **1989**, *28*, 3770–3772. (f) Schaverien, C. J.; Orpen, A. G. *Inorg. Chem.* **1991**, *30*, 4968–4978. (g) Buchler, J. W.; Löffler, J.; Wicholas, M. *Inorg. Chem.* **1992**, *31*, 524–526 and references cited therein. (h) Buchler, J. W.; Scharbert, B. *J. Am. Chem. Soc.* **1988**, *110*, 4272–4276. (i) Horrocks, W. D., Jr.; Hove, E. G. *J. Am. Chem. Soc.* **1978**, *100*, 4386–4392. (j) Lyon, R. C.; Faustino, P. J.; Cohen, J. S.; Katz, A.; Mornex, F.; Colcher, D.; Baglin, C.; Koenig, S. H.; Hambright, P. *Magn. Reson. Med.* **1987**, *4*, 24–33. (k) Megnin, F.; Faustino, P. J.; Lyon, R. C.; Lelkes, P. I.; Cohen, J. S. *Biochem. Biophys. Acta* **1987**, *929*, 173–181. (l) Hambright, P.; Adams, C.; Vernon, K. *Inorg. Chem.* **1988**, *27*, 1660–1662. (m) Haye, S.; Hambright, P. *J. Chem. Soc., Chem. Commun.* **1988**, 666–668. (n) Haye, S.; Hambright, P. *J. Coord. Chem.* **1991**, *22*, 315–320, and references therein. For applications to MRI, see ref 40.

(7) For lanthanide phthalocyanine complexes, see: (a) Kirin, I. S.; Moskalev, P. N.; Makashev, Y. A. *Russ. J. Inorg. Chem. (Engl. Transl.)* **1965**, *10*, 1065–1066. (b) Kasuga, K.; Tsutsui, M.; Petterson, R. C.; Tatsumi, K.; Van Opdenbosch, N.; Pepe, G.; Meyer, E. F., Jr. *J. Am. Chem. Soc.* **1980**, *102*, 4836–4838. (c) Kirin, I. S.; Moskalev, P. N.; Makashev, Y. A. *Russ. J. Inorg. Chem. (Engl. Transl.)* **1967**, *12*, 369–372. (d) MacKay, A. G.; Boas, J. F.; Troup, G. J. *Aust. J. Chem.* **1974**, *27*, 955–964. (e) Chang, A. T.; Marchon, J.-C. *Inorg. Chim. Acta* **1981**, *53*, L241–L243. (f) De Cian, A.; Moussavi, M.; Fischer, J.; Weiss, R. *Inorg. Chem.* **1985**, *24*, 3162–3167. (g) Clarisse, C.; Riou, M. T. *Inorg. Chim. Acta* **1987**, *130*, 139–144. (h) Jiazan, N.; Feng, S.; Zhenxiang, L.; Shaoming, Y. *Inorg. Chim. Acta* **1987**, *139*, 165–168. (i) Kasuga, K.; Nishikori, K.; Mihara, T.; Handa, M.; Sogabe, K.; Isa, K. *Inorg. Chim. Acta* **1990**, *174*, 153–154. (j) Musluoglu, E.; Ahsen, V.; Gul, A.; Bekaroglu, O. *Chem. Ber.* **1991**, *124*, 2531–2536 and references therein.

(8) For some leading references on NMR shift reagents, see: (a) Reuben, J.; Elgavish, G. A. In *Handbook on the Physics and Chemistry of Rare Earths*; Gschneidner, K. A., Jr., Eyring, L., Eds.; North Holland: Amsterdam, 1979; Vol. 4, Chapter 38. (b) Sherry, A. D.; Geraldes, C. F. G. C. In *Lanthanide Probes in Life, Chemical, and Earth Science: Theory and Practice*; Bunzli, J.-C. G., Choppin, G. R., Eds.; Elsevier, New York, 1989; Chapter 4. (c) Sherry, A. D.; Malloy, C. R.; Jeffrey, F. M. H.; Cacheris, W. P.; Geraldes, C. F. G. C. *J. Magn. Reson.* **1988**, *76*, 528–533. (d) Balschi, J. A.; Kohler, S. J.; Bittl, J. A.; Springer, C. S.; Ingwall, J. S. *J. Magn. Reson.* **1989**, *83*, 138. (e) Szklaruk, J.; Marecek, J. F.; Springer, A. L.; Springer, C. S., Jr. *Inorg. Chem.* **1990**, *29*, 660–667. See also ref 16 below.

(9) Luminescent probes: (a) Bunzli, J.-C. G. In ref 8b, Chapter 7, and references therein. (b) Richardson, F. S. *Chem. Rev.* **1982**, *82*, 541–552. (c) Lehn, J.-M.; de Vains, J.-B. R. *Tetrahedron Lett.* **1989**, *30*, 2209–2212. (d) Lehn, J.-M.; Pietraszkiewicz, M.; Karpiuk, J. *Helv. Chim. Acta* **1990**, *73*, 106–111. (e) Lehn, J.-M.; Roth, C. O. *Helv. Chim. Acta* **1991**, *74*, 572–578.

(10) RNA cleavage with lanthanide complexes: (a) Morrow, J. R.; Buttrey, L. A.; Shelton, V. M.; Berback, K. A. *J. Am. Chem. Soc.* **1992**, *114*, 1903–1905 and references therein. (b) Komiyama, M.; Matsumura, K.; Matsumoto, Y. *J. Chem. Soc., Chem. Commun.* **1992**, 640–641. (c) Breslow, R.; Huang, D.-L. *Proc. Natl. Acad. Sci. U.S.A.* **1991**, *88*, 4080–4083.

(11) For reviews of MRI see: (a) Lauffer, R. B. *Chem. Rev.* **1987**, *87*, 901–927. (b) Tweedle, M. F. in ref 8b, pp 127–179. (c) Tweedle, M. F.; Brittain, H. G.; Eckelman, W. C.; Gaughan, G. T.; Hagan, J. J.; Wedeking, P. W.; Runge, V. M. In *Magnetic Resonance Imaging*, 2nd ed.; Partain, C. L., Ed.; Philadelphia, PA, 1988; Vol. 1, pp 793–809. (d) Moonen, C. T.; van-Zijil, P. C.; Frank, J. A.; Le-Bihan, D.; Becker, E. D. *Science* **1990**, *250*, 53–61. (e) Morris, P. G. *Nuclear Magnetic Resonance Imaging in Medicine and Biology*, Claredon Press: Oxford, England, 1986. (f) Murphy, W. A., Jr. *Cancer*, **1991**, *67*, 1169–1176. (g) Nunnally, R. L.; Antich, P. P. *Cancer* **1991**, *67*, 1271–1277. (h) Wagner, H. N. *Cancer* **1991**, *67*, 1121–1128. (i) Ling, G. N.; Kolebic, T.; Damadian, R. *Physiol. Chem. Phys. Med. NMR*, **1990**, *22*, 1–14. (j) Young, S. W. *Magnetic Resonance Imaging: Basic Principles*, Raven Press: New York, 1988, pp 1–282. (k) Edelman, R.; Warach, S. *N. Engl. J. Med.* **1993**, *328*, 708–716.

(12) For leading references of carboxylate-type chelates, see: (a) *Enhanced Magnetic Resonance Imaging*; Runge, V. M., Ed.; C. V. Mosby: St. Louis, MO, 1989. (b) Prasad, J. S.; Okuniewicz, F. J.; Delaney, E. J.; Dischino, D. D. *J. Chem. Soc., Perkin Trans. 1* **1991**, 3329–3332. (c) Aime, S.; Botta, M.; Ermondi, G.; Fedeli, F.; Uggeri, F. *Inorg. Chem.* **1992**, *31*, 1100–1103, and references cited therein. (d) Chang, C. A. *Eur. J. Solid State Inorg. Chem.* **1991**, *28*, 237–244. (e) Forsberg, J. H.; Moeller, T. In *Gmelin Handbook of Inorganic Chemistry*; Springer-Verlag: Berlin, 1980; Vol. D1, pp 160 and 200.

(13) For relevant DTPA-related references, see: (a) Tweedle, M. F.; Gaughan, G. T.; Hagan, J.; Wedeking, P. W.; Sibley, P.; Wilson, L. J.; Lee, D. W. *Nucl. Med. Biol.* **1988**, *15*, 31. (b) Konings, M. S.; Dow, W. C.; Love, D. B.; Raymond, K.; Quay, S. C.; Rocklage, S. M. *Inorg. Chem.* **1990**, *29*, 1488–1491. (c) Armitage, F. E.; Richardson, D. E.; Li, K. C. P. *Bioconjugate Chem.* **1990**, *1*, 365–374. (d) Geraldes, C. F. G. C.; Urbano, A. M.; Alpiom, M. C.; Hoefnagel, M. A.; Peters, J. A. *J. Chem. Soc., Chem. Commun.* **1991**, 656–658. (e) Spirlet, M.-R.; Rebizant, J.; Loncin, M.-F.; Desreux, J. F. *Inorg. Chem.* **1984**, *23*, 4278–4283.

(14) For leading references to relevant DOTA and DO3A complexes, see: (a) Loncin, M. F.; Desreux, J. F.; Merciny, E. *Inorg. Chem.* **1986**, *25*, 2646–2648. (b) Brucher, E.; Laurenczy, G.; Makra, Z. S. *Inorg. Chim. Acta* **1987**, *139*, 141–142. (c) Cacheris, W. P.; Nickle, S. K.; Sherry, A. D. *Inorg. Chem.* **1987**, *26*, 958–960. (d) Clarke, E. T.; Martell, A. E. *Inorg. Chim. Acta* **1991**, *190*, 37–46. (e) Wang, X.; Jin, T.; Comblin, V.; Lopez-Mut, A.; Merciny, E.; Desreux, J. F. *Inorg. Chem.* **1992**, *31*, 1095–1099 and references therein. (f) Aime, S.; Botta, M.; Ermondi, G.; Fedeli, F.; Uggeri, F. *Inorg. Chem.* **1992**, *31*, 1100–1103. (g) Dischino, D. D.; Delaney, E. J.; Emswiler, J. E.; Gaughan, G. T.; Prasad, J. S.; Srivastava, S. K.; Tweedle, M. F. *Inorg. Chem.* **1991**, *30*, 1265–1269. (h) Zhang, X.; Chang, C. A.; Brittain, H. G.; Garrison, J. M.; Telser, J.; Tweedle, M. F. *Inorg.* **1993**, *32*, 587–593.

(15) For a review of "expanded porphyrins," see: Sessler, J. L.; Burrell, A. K. *Top. Curr. Chem.* **1991**, *161*, 177–273.

(16) (a) Sessler, J. L.; Murai, T.; Lynch, V.; Cyr, M. *J. Am. Chem. Soc.* **1988**, *110*, 5586–5588. (b) Sessler, J. L.; Murai, T.; Lynch, V. *Inorg. Chem.* **1989**, *28*, 1333–1341. (c) Maiya, B. G.; Mallouk, T. E.; Hemmi, G.; Sessler, J. L. *Inorg. Chem.* **1990**, *29*, 3738–3745.

Chart I

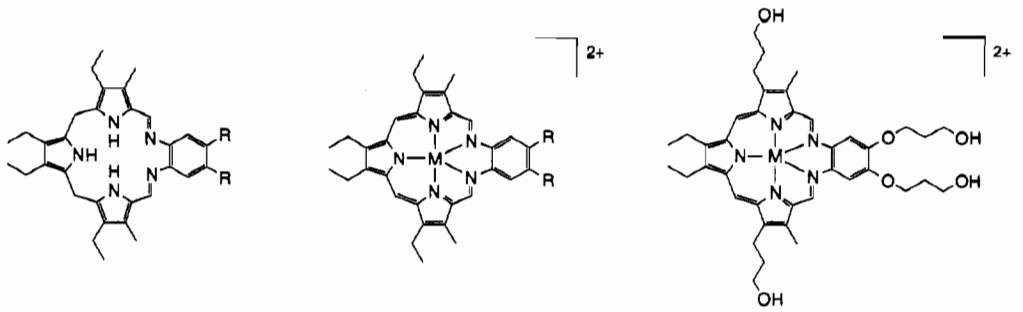

45 R = OCH_3
46 R = $O(CH_2)_3OH$

1	M = Gd,	R = CH_3
2	M = H,	R = OCH_3
3	M = La,	R = OCH_3
4	M = Ce,	R = OCH_3
5	M = Pr,	R = OCH_3
6	M = Nd,	R = OCH_3
7	M = Sm,	R = OCH_3
8	M = Eu,	R = OCH_3
9	M = Gd,	R = OCH_3
10	M = Tb,	R = OCH_3
11	M = Dy,	R = OCH_3
12	M = Ho,	R = OCH_3
13	M = Er,	R = OCH_3
14	M = Tm,	R = OCH_3
15	M = Yb,	R = OCH_3
16	M = Lu,	R = OCH_3
21	M = H,	R = $O(CH_2)_3OH$
22	M = Lu,	R = $O(CH_2)_3OH$

30 M = H
31 M = La
32 M = Ce
33 M = Pr
34 M = Nd
35 M = Sm
36 M = Eu
37 M = Gd
38 M = Tb
39 M = Dy
40 M = Ho
41 M = Er
42 M = Tm
43 M = Yb
44 M = Lu

gadolinium(III) texaphyrin complex, **1**.[17] Although no X-ray structural information was obtained and although this material proved insoluble in water, detailed kinetic studies carried out in 1:1 water–methanol indicated that the half-life for decomplexation and/or decomposition was 37 days. Encouraged by these results, we sought to prepare a new type of analogous gadolinium(III) texaphyrin complex that would be soluble in water and which could, therefore, perhaps have use as a possible MRI contrast agent. Here, we wish to present the synthesis and X-ray structural characterization of such a water soluble gadolinium(III) texaphyrin complex, namely **37**, which is of interest to us as a possible improved contrast agent.[18] We also wish to report the synthesis of a full range of lanthanide(III) texaphyrin complexes (i.e., **3–16**, **22**, **31–44**), including four (**3**, **9**, **22**, and **36**) that were characterized by X-ray diffraction. Aspects of this chemistry have been communicated elsewhere.[18] Structures are given in Chart I.

Experimental Section

General Information. ^1H and ^{13}C NMR spectra were obtained on a General Electric QE-300, Bruker AC-250, or Bruker AM-500 spectrometer. Electronic spectra were recorded on a Beckman DU-7 spectrophotometer in MeOH. Infrared spectra were recorded, as KBr pellets, from 4000 to 800 cm^{-1} on a Nicolet 510P FT-IR spectrophotometer. Routine low-resolution electron impact mass spectra (EI MS) were measured with a Bell and Howell 21-110B. Low-resolution chemical ionization (CI) and fast atom bombardment (FAB MS) were performed with a Finnigan-MAT TSQ-70. All high-resolution mass spectra were performed on a VG ZAB-2E instrument. 3-Nitrobenzyl alcohol or glycerol was used as the matrix for FAB mass spectra. Elemental analyses were performed by Atlantic Microlabs, Inc with all samples being predried *in vacuo* prior to analysis. Melting points were measured on a Mel-temp apparatus and are uncorrected.

Materials. All solvents were of reagent grade quality and purchased commercially. Tetrahydrofuran (THF) was dried over Na/benzophenone and CH_2Cl_2 was dried over CaH_2. Merck Type 60 (230–400 mesh) silica gel and Brockmann I activated neutral alumina (150 mesh) were used for column chromatography. Thin layer chromatography (TLC) was carried out using 10% methanol in chloroform as the eluent on Whatman K6F silica gel plates.

General Procedure for the Synthesis of Lanthanide(III) Complexes of 4,5,9,24-Tetraethyl-16,17-dimethoxy-10,23-dimethyl-13,20,25,26,27-pentaazapentacyclo[20.2.1.1^{3,6}.1^{8,11}.0^{14,19}]heptacosa-1,3,5,7,9,11(27),12,14,16,18,20,22(25),23-tridecaene (2).[19] One equivalent of the protonated form of the macrocycle, 4,5,9,24-tetraethyl-16,17-dimethoxy-10,23-dimethyl-13,20,25,26,27-pentaazapentacyclo[20.2.1.1^{3,6}.1^{8,11}.0^{14,19}]-heptacosa-3,5,8,10,12,14(19),15,17,20,22,24-undecaene[19] (**45**), 3 equiv of the $Ln(NO_3)_3 \cdot xH_2O$ metal salt, and triethylamine (ca. 1 mL) were mixed together in methanol and heated to reflux under air. The progression of the reaction was monitored by UV/vis spectroscopy. After completion, the reaction was cooled to room temperature, the solvent removed under reduced pressure, and the resulting green solid dried *in vacuo* overnight. The complex was purified by column chromatography through silica gel using chloroform containing increasing amounts of methanol (0–15%) as the eluent. After the initial red fraction was discarded, the green complex was generally eluted off the column with 5–10% methanol in chloroform. Fractions containing the complex were combined and the solvent reduced to dryness. The complex was dissolved into methanol (ca. 50 mL), diluted with 100 mL of CH_2Cl_2, and washed with 1 M aqueous $NaNO_3$ (2 × 50 mL). If the complex precipitated during the wash, more methanol was added to redissolve the complex. The organic layer was separated and the water wash extracted once with CH_2Cl_2. The various organic layers were then combined and filtered through a pad of Celite, using methanol to wash the complex completely through the Celite. The solvent was then removed under reduced pressure and the complex dried *in vacuo* overnight. The complex was recrystallized from methanol/CH_2Cl_2/diethyl ether.

Lanthanum(III) Complex 3. The protonated form of macrocycle **45** (300 mg, 0.51 mmol), $La(NO_3)_3 \cdot 6H_2O$ (708 mg), and triethylamine (ca. 1 mL) in methanol (300 mL) were heated at reflux under air for 2 h. After workup using the general procedure described above, 107 mg of the complex was obtained (26%). Single crystals suitable for X-ray diffraction analysis were obtained by dissolving the purified complex in a mixture of MeOH/$CHCl_3$, while inducing crystallization by vapor diffusion of diethyl ether. ^1H NMR ($CD_3OD/CDCl_3$, $CDCl_3$ as reference): δ 1.43 (t, 6H, CH_2CH_3), 1.48 (t, 6H, CH_2CH_3), 3.01 (s, 6H, pyrr-CH_3), 3.41–3.52 (m, 8H, CH_2CH_3), 4.28 (s, 6H, Ph-OCH_3), 9.02 (s, 2H, Ph-H), 9.58 (s, 2H, $(pyrr)_2CH$), 11.43 (s, 2H, HC=N). ^{13}C NMR ($CD_3OD/CDCl_3$, CD_3OD as reference): δ 10.9, 17.7, 18.8, 20.0, 20.1, 57.6, 100.2, 117.6, 136.1, 139.9, 144.0, 147.1, 147.4, 150.1, 152.5,

(17) Sessler, J. L.; Hemmi, G.; Murai, T. *Inorg. Chem.* **1989**, *28*, 3390–3393.
(18) Sessler, J. L.; Mody, T. D.; Hemmi, G. W.; Young, S. W.; Miller, R. A. *J. Am. Chem. Soc.*, submitted for publication.
(19) Sessler, J. L.; Mody, T. D.; Ramasamy, R.; Sherry, A. D. *New J. Chem.* **1992**, *16*, 541–544.

154.9, 159.1. UV/vis (CH_3OH) [λ_{max}, nm (log ϵ)]: 346.5 (4.33), 415.5 (4.68), 473.0 (5.01), 743.0 (4.55). FAB MS, M^+: *m/e* 687 (for ^{139}La). HR MS, M^+: *m/e* 687.2076 (calcd for $C_{34}H_{38}N_5O_2{}^{139}La$, 687.2089). Anal. Calcd for $[C_{34}H_{38}N_5O_2La](NO_3)_2$: C, 50.32; H, 4.72; N, 12.08. Found: C, 50.05; H, 4.75; N, 11.98. This complex was further characterized by X-ray diffraction analysis.

Cerium(III) Complex 4. The protonated form of macrocycle **45** (150 mg, 0.25 mmol), $Ce(NO_3)_3{\cdot}6H_2O$ (353 mg), and triethylamine (ca. 1 mL) in methanol (150 mL) were heated at reflux for 10 h. After workup using the general procedure described above, 59 mg of the complex was obtained (28%). UV/vis (CH_3OH) [λ_{max}, nm (log ϵ)]: 348.5 (4.29), 415.5 (4.63), 472.5 (4.98), 741.5 (4.51). FAB MS, M^+: *m/e* 688 (for ^{140}Ce). HR MS, M^+: *m/e* 688.2061 (calcd for $C_{34}H_{38}N_5O_2{}^{140}Ce$, 688.2080). Anal. Calcd for $[C_{34}H_{38}N_5O_2Ce](NO_3)_2H_2O$: C, 49.15; H, 4.85; N, 11.80. Found: C, 49.39; H, 4.77; N, 11.68.

Praseodymium(III) Complex 5. The protonated form of macrocycle **45** (150 mg, 0.25 mmol), $Pr(NO_3)_3{\cdot}5H_2O$ (339 mg), and triethylamine (ca. 1 mL) in methanol (150 mL) were heated at reflux for 9 h. After workup using the general procedure described above, 63 mg of the complex was obtained (30%). UV/vis (CH_3OH) [λ_{max}, nm (log ϵ)]: 350.0 (4.26), 415.5 (4.59), 473.5 (4.93), 742.0 (4.47). FAB MS, M^+: *m/e* 690 (for ^{141}Pr). HR MS, M^+: *m/e* 689.2095 (calcd for $C_{34}H_{38}N_5O_2{}^{141}Pr$, 689.2102). Anal. Calcd for $[C_{34}H_{38}N_5O_2Pr](NO_3)_2(CH_3OH)_{1/2}$: C, 49.95; H, 4.86; N, 11.82. Found: C, 50.17; H, 4.95; N, 11.40.

Neodymium(III) Complex 6. The protonated form of macrocycle **45** (150 mg, 0.25 mmol), $Nd(NO_3)_3{\cdot}5H_2O$ (272 mg), and triethylamine (ca. 1 mL) in methanol (150 mL) were heated at reflux for 12 h. After workup using the general procedure described above, 106 mg of the complex was obtained (50%). UV/vis (CH_3OH) [λ_{max}, nm (log ϵ)]: 348.5 (4.27), 414.5 (4.61), 473.0 (4.97), 741.0 (4.50). FAB MS, M^+: *m/e* 691 (for ^{142}Nd). HR MS, M^+: *m/e* 690.2103 (calcd for $C_{34}H_{38}N_5O_2{}^{142}Nd$, 690.2103). Anal. Calcd for $[C_{34}H_{38}N_5O_2Nd](NO_3)_2(CH_3OH)_{1/2}$: C, 49.75; H, 4.84; N, 11.77. Found: C, 49.22; H, 4.80; N, 11.75.

Samarium(III) Complex 7. The protonated form of macrocycle **45** (150 mg, 0.25 mmol), $Sm(NO_3)_3{\cdot}5H_2O$ (349 mg), and triethylamine (ca. 1 mL) in methanol (150 mL) were heated at reflux for 10 h. After workup using the general procedure described above, 119 mg of the complex was obtained (56%). UV/vis (CH_3OH) [λ_{max}, nm (log ϵ)]: 416.5 (4.60), 472.5 (4.97), 738.0 (4.50). FAB MS, M^+: *m/e* 700 (for ^{152}Sm). HR MS, M^+: *m/e* 700.2203 (calcd for $C_{34}H_{38}N_5O_2{}^{152}Sm$, 700.2223). Anal. Calcd for $[C_{34}H_{38}N_5O_2Sm](NO_3)_2H_2O$: C, 48.55; H, 4.79; N, 11.66. Found: C, 48.78; H, 4.79; N, 11.62.

Europium(III) Complex 8. The protonated form of macrocycle **45** (150 mg, 0.25 mmol), $Eu(NO_3)_3{\cdot}6H_2O$ (363 mg), and triethylamine (ca. 1 mL) in methanol (150 mL) were heated at reflux for 10 h. After workup using the general procedure described above, 102 mg of the complex was obtained (49%). UV/vis (CH_3OH) [λ_{max}, nm (log ϵ)]: 350.0 (4.30), 413.5 (4.64), 472.5 (4.99), 682.5 (3.99), 736.5 (4.53). FAB MS, M^+: *m/e* (relative intensity) 699 (^{151}Eu, 88), 701 (^{153}Eu, 100). HR MS, M^+: *m/e* 699.2224 (calcd for $C_{34}H_{38}N_5O_2{}^{151}Eu$, 699.2224). Anal. Calcd for $[C_{34}H_{38}N_5O_2Eu](NO_3)_2$: C, 49.52; H, 4.64; N, 11.89. Found: C, 49.45; H, 4.61; N, 11.77.

Gadolinium(III) Complex 9. The protonated form of macrocycle **45** (291 mg, 0.49 mmol), $Gd(NO_3)_3{\cdot}5H_2O$ (686 mg), and triethylamine (ca. 1 mL) in methanol (300 mL) were heated at reflux for 7 h. After workup using the general procedure described above, 256 mg of the complex was obtained (63%). UV/vis (CH_3OH) [λ_{max}, nm (log ϵ)]: 352.0 (4.34), 413.0 (4.67), 472.0 (5.04), 681.5 (4.04), 735.0 (4.58). FAB MS, $[M - H]^+$: *m/e* 705 (for ^{158}Gd). HR MS, M^+: *m/e* 706.2243 (calcd for $C_{34}H_{38}N_5O_2{}^{158}Gd$, 706.2267). Anal. Calcd for $[C_{34}H_{38}N_5O_2Gd](NO_3)_2(CH_3OH)(H_2O)$: C, 47.77; H, 5.04; N, 11.14. Also calcd for $[C_{34}H_{38}N_5O_2Gd](NO_3)_2(CH_3OH)_{3/2}(H_2O)_{1/2}$: C, 48.07; H, 5.11; N, 11.05. Found: C, 47.80; H, 5.03; N, 10.79.

Terbium(III) Complex 10. The protonated form of macrocycle **45** (150 mg, 0.25 mmol), $Tb(NO_3)_3{\cdot}5H_2O$ (368 mg), and triethylamine (ca. 1 mL) in methanol (150 mL) were heated at reflux for 20 h. After workup using the general procedure described above, 113 mg of the complex was obtained (52%). UV/vis (CH_3OH) [λ_{max}, nm (log ϵ)]: 352.5 (4.27), 412.0 (4.60), 472.5 (4.96), 678.0 (3.96), 733.0 (4.50). FAB MS, M^+: *m/e* 708 (for ^{159}Tb). HR MS, M^+: *m/e* 707.2280 (calcd for $C_{34}H_{38}N_5O_2{}^{159}Tb$, 707.2279). Anal. Calcd for $[C_{34}H_{38}N_5O_2Tb](NO_3)_2H_2O$: C, 48.06; H, 4.75; N, 11.54. Found: C, 47.66; H, 4.50; N, 11.57.

Holmium(III) Complex 12. The protonated form of macrocycle **45** (150 mg, 0.25 mmol), $Ho(NO_3)_3{\cdot}5H_2O$ (414 mg), and triethylamine (ca. 1 mL) in methanol (150 mL) were heated at reflux for 10 h. After workup using the general procedure described above, 132 mg of the complex was obtained (61%). UV/vis (CH_3OH) [λ_{max}, nm (log ϵ)]: 354.0 (4.29), 413.0 (4.62), 473.0 (4.99), 672.0 (3.96), 730.5 (4.53). FAB MS, M^+: *m/e* 714 (for ^{165}Ho). HR MS, M^+: m/e 713.2315 (calcd for $C_{34}H_{38}N_5O_2{}^{165}Ho$, 713.2329). Anal. Calcd for $[C_{34}H_{38}N_5O_2Ho](NO_3)_2{\cdot}H_2O$: C, 47.73; H, 4.71; N, 11.46. Found: C, 47.33; H, 4.42; N, 11.40.

Erbium(III) Complex 13. The protonated form of macrocycle **45** (150 mg, 0.25 mmol), $Er(NO_3)_3{\cdot}5H_2O$ (360 mg), and triethylamine (ca. 1 mL) in methanol (150 mL) were heated at reflux for 20 h. After workup using the general procedure described above, 113 mg of the complex was obtained (52%). UV/vis (CH_3OH) [λ_{max}, nm (log ϵ)]: 354.0 (4.33), 413.0 (4.67), 474.5 (5.04), 670.0 (4.00), 730.0 (4.58). FAB MS, M^+: *m/e* 715 (for ^{166}Er). HR MS, M^+: *m/e* 714.2308 (calcd for $C_{34}H_{38}N_5O_2{}^{166}Er$, 714.2329). Anal. Calcd for $[C_{34}H_{38}N_5O_2Er](NO_3)_2H_2O$: C, 47.60; H, 4.70; N, 11.43. Found: C, 47.43; H, 4.44; N, 11.20.

Thulium(III) Complex 14. The protonated form of the macrocycle **45** (150 mg, 0.25 mmol), $Tm(NO_3)_3{\cdot}5H_2O$ (366 mg), and triethylamine (ca. 1 mL) in methanol (150 mL) were heated at reflux for 11 h. After workup using the general procedure described above, 126 mg of the complex was obtained (59%). UV/vis (CH_3OH) [λ_{max}, nm (log ϵ)]: 356.0 (4.31), 414.0 (4.66), 475.0 (5.04), 669.0 (3.98), 729.5 (4.57). FAB MS, M^+: *m/e* 717 (for ^{169}Tm); HR MS, M^+: m/e 717.2365 (calcd for $C_{34}H_{38}N_5O_2{}^{169}Tm$, 717.2368). Anal. Calcd for $[C_{34}H_{38}N_5O_2Tm](NO_3)_2$: C, 48.52; H, 4.55; N, 11.65. Found: C, 48.61; H, 4.57; N, 11.49.

Ytterbium(III) Complex 15. The protonated form of macrocycle **45** (150 mg, 0.25 mmol), $Yb(NO_3)_3{\cdot}5H_2O$ (406 mg), and triethylamine (ca. 1 mL) in methanol (150 mL) were heated at reflux for 11 h. After workup using the general procedure described above, 130 mg of the complex was obtained (60%). UV/vis (CH_3OH) [λ_{max}, nm (log ϵ)]: 357.0 (4.29), 414.0 (4.64), 475.0 (5.01), 668.0 (3.95), 729.0 (4.54). FAB MS, M^+: *m/e* 720 (for ^{171}Yb); HR MS, M^+: m/e 719.2405 (calcd for $C_{34}H_{38}N_5O_2{}^{171}Yb$, 719.2389). Anal. Calcd for $[C_{34}H_{38}N_5O_2Yb](NO_3)_2$: C, 48.29; H, 4.53; N, 11.59. Found: C, 48.78; H, 4.56; N, 11.07.

Lutetium(III) Complex 16. The protonated form of macrocycle **45** (300 mg, 0.51 mmol), $Lu(NO_3)_3{\cdot}xH_2O$ (588 mg), and triethylamine (ca. 1 mL) in methanol (300 mL) were heated at reflux for 11 h. After workup using the general procedure described above, 204 mg of the complex was obtained (47%). UV/vis (CH_3OH) [λ_{max}, nm (log ϵ)]: 355.5 (4.29), 413.5 (4.65), 474.5 (5.00), 668.5 (3.91), 728.0 (4.52). FAB MS, M^+: *m/e* 723 (for ^{175}Lu). HR MS, M^+: *m/e* 723.2451 (calcd for $C_{34}H_{38}N_5O_2{}^{175}Lu$, 723.2433). Anal. Calcd for $[C_{34}H_{38}N_5O_2Lu](NO_3)_2$: C, 48.18; H, 4.52; N, 11.57. Found: C, 48.04; H, 4.54; N, 11.40.

Preparation of Water Soluble Texaphyrins. 1,2-Bis(2-carboxyethoxy)-4,5-dinitrobenzene (18). To a well-stirred solution of *o*-bis((3-hydroxypropyl)oxy)benzene[20] (**17**) (5.0 g, 22 mmol) in 30 mL of glacial acetic acid cooled to 15 °C was added 20 mL of concentrated nitric acid (70%) dropwise over a period of 15 min. The temperature was held below 40 °C by cooling and proper regulation of the rate of acid addition. After the addition, the yellow solution stirred at room temperature for 15 min. Here, the solution was cooled again to 15 °C and 50 mL of fuming nitric acid (90%) was added dropwise over a period of 30 min. The orange solution was brought to room temperature and it stirred for approximately 48 h. After 48 h, the reaction solution was checked by TLC, which displayed only one low R_f spot, which corresponds to the diacid. Therefore, the orange solution was poured onto 600 mL of ice in a 1 L beaker. The precipitated dinitro product was filtered, washed with water (1000 mL) until free from acid and dried *in vacuo* for 24 h. The crude product was recrystallized from acetone/*n*-hexanes to yield the diacid as fluffy yellow needles (4.20 g, 55.2%), mp: 166–167 °C. ^1H NMR (acetone-d_6): δ 2.87 (t, 4H, $OCH_2CH_2CO_2H$), 4.49 (t, 4H, $OCH_2CH_2CO_2H$), 7.71 (s, 2H, Ar-H), 9–10 (br s, 2H, CO_2H). ^{13}C NMR (acetone-d_6): δ 33.76, 66.57, 109.85, 137.14, 152.06, 171.51. EI MS: *m/e* (relative intensity) 344 (100). HRMS (M^+): *m/e* 344.0492 (calcd. for $C_{12}H_{12}N_2O_{10}$: 344.0493).

1,2-Bis((3-hydroxypropyl)oxy)-4,5-dinitrobenzene (19). In a dry 500-mL round-bottom flask, equipped with a 125-mL pressure-equalized dropping funnel, 1,2-bis((2-carboxy)ethoxy)-4,5-dinitrobenzene **18** (5.0 g, 14.5 mmol) was dissolved in 50 mL of dry THF (distilled over ketyl) and stirred at 0–10 °C under nitrogen. To the resulting clear solution

(20) Kyba, E. P.; Davis, R. E.; Hudson, C. W.; John, A. M.; Brown, S. B.; McPhaul, L.-K.; Glover, A. C. *J. Am. Chem. Soc.* **1981**, *103*, 3868–3875.

was added 120 mL of $(BH_3)_2$·THF (1 M) dropwise over a period of 30 min. After the borane–THF addition, the reaction mixture was stirred an additional 5 min at 10 °C and then it was brought up to room temperature. The formation of the diol product was followed by TLC and the reaction was deemed complete after approximately 2 h. The diborane solution was quenched by careful addition of 65 mL of absolute methanol (*careful: frothing occurs*). After the yellow solution was stirred for 30 min, it was concentrated to a bright yellow solid on a rotary evaporator. The crude solid was dissolved in 200 mL of ethyl acetate and washed with 4 M sodium acetate (2 × 100 mL), water (2 × 100 mL) and then brine (50 mL). The organic layer was dried over $MgSO_4$ and concentrated to dryness on a rotary evaporator. The crude product was recrystallized from acetone/*n*-hexanes to afford 4.12 g (90%) of orange needles, mp 129–130 °C. ^{1}H NMR ($CDCl_3/CD_3OD$): δ 2.10 (p, 4H, $OCH_2CH_2CH_2OH$), 3.81 (t, 4H, $OCH_2CH_2CH_2OH$), 4.28 (t, 4H, $OCH_2CH_2CH_2OH$), 7.41 (s, 2H, ArH). ^{13}C NMR (acetone-d_6): δ 32.52, 58.50, 67.81, 107.88, 137.03, 152.47. EI MS: *m/e* (relative intensity) 316 (100). HRMS (M^+): *m/e* 316.0914 (calcd for $C_{12}H_{16}N_2O_8$, 316.0907).

1,2-Diamino-4,5-bis((3′-hydroxypropyl)oxy)benzene (20). The diamine was obtained by reduction of the corresponding 1,2-bis((3-hydroxypropyl)oxy)-4,5-dinitrobenzene **19** (3.0 g, 9.6 mmol) with hydrazine hydrate (4.7 mL, 96.2 mmol) and 10% palladium on carbon (200 mg) in 120 mL of refluxing absolute ethanol. The resulting brown suspension bubbled for approximately 15–20 min and then turned colorless after 1 h. At this point, the reduction was deemed complete as judged by TLC (a low R_f spot). The reaction solution was hot-filtered through Celite into a dry flask, covered with aluminum foil, and then concentrated to a gray solid. The diamine was recrystallized from hot acetone to yield 2.20 g (91%) of an off-white fine powder, mp 115–117 °C. ^{1}H NMR (DMSO-d_6): δ 1.76 (p, 4H, $OCH_2CH_2CH_2OH$), 3.53 (q, 4H, $OCH_2CH_2CH_2OH$), 3.82 (t, 4H, $OCH_2CH_2CH_2OH$), 4.06 (s, 4H, NH), 4.44 (t, 2H, OH), 6.25 (s, 2H, ArH). ^{13}C NMR (DMSO-d_6): δ 42.68, 67.84, 77.08, 114.95, 139.01, 150.63. EI MS: *m/e* (rel. intensity) 256 (100). HRMS (M^+): *m/e* 256.1420 (calcd for $C_{12}H_{20}N_2O_4$, 256.1423).

4,5,9,24-Tetraethyl-16,17-bis((3-hydroxypropyl)oxy)-10,23-dimethyl-13,20,25,26,27-pentaazapentacyclo[20.2.1.1^{3,6}.1^{8,11}.0^{14,19}]heptacosa-3,5,8,-10,12,14(19),15,17,20,22,24-undecaene (46). In a 500-mL round-bottom flask (oven dried) 2,5-bis((3-ethyl-5-formyl-4-methylpyrrol-2-yl)methyl)-3,4-diethylpyrrole[21] (100 mg, 0.238 mmol) and 1,2-diamino-4,5-bis((3-hydroxypropyl)oxy)benzene **20** (60 mg, 0.238 mmol) were combined with 250 mL of anhydrous toluene and 50 mL of absolute methanol under nitrogen. Concentrated HCl (3 drops) was added, and the resulting solution was heated to reflux for 2 h. The red solution was cooled to room temperature and then concentrated to dryness under reduced pressure. The hydrochloride salt of the sp^3 texaphyrin was recrystallized from dichloromethane/*n*-hexanes to yield 150 mg (93%) of a crimson red solid, mp 190 °C dec. ^{1}H NMR ($CDCl_3$): δ 1.05 (t, 6H, CH_2CH_3), 1.12 (t, 6H, CH_2CH_3), 2.00 (t, 4H, $OCH_2CH_2CH_2OH$), 2.28 (s, 6H, pyrr-CH_3), 2.35 (q, 4 H, CH_2CH_3), 2.48 (q, 4H, CH_2CH_3), 3.00–3.50 (bs, 2H, OH), 3.78 (t, 4H, $OCH_2CH_2CH_2OH$), 3.93 (s, 4H, (pyrr)$_2$-CH_2), 4.19 (t, 4H, $OCH_2CH_2CH_2OH$), 7.16 (s, 2H, ArH), 8.34 (s, 2H, HC=N), 11.16 (s, 1H, NH), 12.04 (s, 2H, NH). ^{13}C NMR ($CDCl_3$): δ 9.65, 15.45, 16.61, 17.23, 17.60, 22.18, 31.71, 60.75, 68.58, 100.86, 120.23, 120.37, 124.97, 125.06, 130.05, 133.86, 140.16, 140.86, 147.62; UV/vis λ_{max} (MeOH) 369 nm; CI MS (M+H) 643; CI HRMS (M+H) 642.4039 (calcd. for $C_{38}H_{52}N_5O_4$ 642.4019).

Lutetium(III) Complex of 4,5,9,24-Tetraethyl-16,17-bis((3-hydroxypropyl)oxy)-10,23-dimethyl-13,20,25,26,27-pentaazapentacyclo-[20.2.1.1^{3,6}.1^{8,11}.0^{14,19}]heptacosa-1,3,5,7,9,11(27),12,14(19),15,17,20,22-(25),23-tridecaene 21 (22). The hydrochloride salt of 4,5,9,24-tetraethyl-16,17-bis((3-hydroxypropyl)oxy)-10,23-dimethyl-13,20,25,26,27-pentaazapentacyclo-[20.2.1.1^{3,6}.1^{8,11}.0^{14,19}]heptacosa-3,5,8,10,-12,14(19),15,17,20,22,24-undecaene (**46**) (100 mg, 0.15 mmol), Lu-$(NO_3)_3$·H_2O (177 mg, 0.47 mmol), and triethylamine (ca. 0.5 mL) were combined in 150 mL of refluxing methanol for 24 h. The dark green reaction mixture was concentrated on a rotary evaporator to dryness and dried *in vacuo* for 24 h. The crude complex was dissolved in a 100 mL 1:1 (v/v) mixture of chloroform and methanol, filtered through Celite, and concentrated to 20 mL. A small amount of silica gel (approximately 3 g) was added to the flask and then the dark green solution was carefully concentrated to dryness on a rotary evaporator. The silica was dried for 2 h *in vacuo*, then it was loaded on a chloroform packed silica column and the complex was purified by first using neat chloroform and then increasing concentrations of methanol in chloroform (0–20%) as eluents. The dark green band collected from the column was concentrated to dryness on a rotary evaporator and recrystallized from chloroform/methanol/diethyl ether to yield 50 mg (ca. 37%) of the lutetium(III) texaphyrin. ^{1}H NMR ($CDCl_3/CD_3OH$): δ 1.82–1.91 (m, 12H, CH_2CH_3), 2.39 (m, 4H, $OCH_2CH_2CH_2OH$), 3.32 (m, 4H, $OCH_2CH_2CH_2OH$), 3.39 (s, 6H, pyrr-CH_3), 3.92–4.04 (m, 12H, $OCH_2CH_2CH_2OH$ and CH_2CH_3), 3.93 (s, 4H, (pyrr)$_2$-CH_2), 9.52 (s, 2H, CH=C), 10.24 (s, 2H, ArH), 12.23 (s, 2H, HC=N). UV/vis [λ_{max}, nm (MeOH)]: 420.0, 477.5, 730.0. FAB MS, M^+: *m/e* 809; HRMS, M^+: *m/e* 809.2791 (calcd for $C_{38}H_{44}N_5O_4{}^{175}Lu$, 809.2801). X-ray quality crystals were obtained by dissolving the Lu(III) complex in a mixture of warm $CHCl_3$ and MeOH and then allowing diethyl ether to diffuse into the cooled solution.

2,5-Bis[(5-((benzyloxy)carbonyl)-3-((methoxycarbonyl)ethyl)-4-methylpyrrol-2-yl)methyl]-3,4-diethylpyrrole (25). Ethanol (absolute, 250 mL), from an unopened bottle, was placed in a 500-mL round-bottom flask and purged with dry nitrogen for 10 min. 2-(Acetoxymethyl)-5-((benzyloxy)carbonyl)-4-methyl-3-((methoxycarbonyl)ethyl)pyrrole[22] (**23**) (7.83 g, 0.02 mol) and 3,4-diethylpyrrole[23] (**24**) (1.29 g, 0.01 mol) were added and the mixture heated at 60 °C until all of the pyrroles dissolved. *p*-Toluenesulfonic acid (65 mg) was added and the reaction temperature maintained at 60 °C. The reaction slowly changed color from a clear yellow to a dark red with the product precipitating out of the solution as the reaction progressed. After 10 h, the reaction was cooled to room temperature, the solvent volume reduced to half its volume on the rotary evaporator, and the resulting slurry placed in the freezer for several hours. The product was collected by filtration and washed with a small amount of cold ethanol to afford 5.63 g of an off-white fine powder (75%), mp 159–160 °C; ^{1}H NMR ($CDCl_3$): δ 1.14 (t, 6H, CH_2CH_3), 2.23 (s, 6H, pyrr-CH_3), 2.31 (t, 4H, $CH_2CH_2CO_2CH_3$), 2.50 (q, 4H, CH_2CH_3), 2.64 (t, 4H, $CH_2CH_2CO_2CH_3$), 3.60 (br s, 10H, CH_3CO_2- and (pyrr)$_2$-CH_2), 4.44 (br s, 4H, $C_6H_5CH_2$), 6.99–7.02 (m, 4H, PhH), 7.22–7.26 (m, 6H, PhH), 8.72 (s, 1H, NH), 10.88 (br s, 2H, NH); ^{13}C NMR ($CDCl_3$): δ 11.0, 16.8, 17.7, 19.4, 22.1, 35.1, 51.5, 65.3, 117.4, 119.3, 122.1, 126.6, 126.8, 127.4, 128.2, 133.5, 136.6, 162.4, 173.5. CI MS, $(M + H)^+$: *m/e* 750. HR MS, M^+: *m/e* 749.3676 (calcd for $C_{44}H_{51}N_3O_8$, 749.3676).

2,5-Bis[(5-((benzyloxy)carbonyl)-3-(3-hydroxypropyl)-4-methylpyrrol-2-yl)methyl]-3,4-diethylpyrrole (26). 2,5-Bis[(5-((benzyloxy)carbonyl)-4-methyl-3-(methoxycarbonyl)ethyl)pyrrol-2-yl)methyl]-3,4-diethylpyrrole **25** (5.00 g, 0.007 mol) was placed in a three-necked 100-mL round-bottom flask and vacuum dried for ca. 30 min. The flask was equipped with an addition funnel, a thermometer, a nitrogen inlet tube, and a magnetic stir bar. After the tripyrrane was partially dissolved into 10 mL of dry THF, 29 mL of borane (1 M BH_3 in THF) was added dropwise with stirring. The reaction became mildly exothermic and was cooled with a cool water bath. The tripyrrane slowly dissolved to form a homogeneous orange solution which turned a bright fluorescent orange color as the reaction went to completion. After being stirred for 1 h at room temperature, the reaction was quenched by adding methanol dropwise until the vigorous effervescence ceased. The solvents were removed under reduced pressure, and the resulting white solid was redissolved into CH_2Cl_2. The tripyrrane solution was washed three times with 0.5 M HCl (200 mL total), dried over anhydrous K_2CO_3, and filtered. The solvent was concentrated to a small volume under reduced pressure, then hexanes (50 mL) was added. The tripyrrane was allowed to crystallize in the freezer for several hours. The product was filtered and again recrystallized from CH_2Cl_2/ethanol. The product was collected by filtration and vacuum dried to yield 4.12 g of an orange-tinted white solid (85%), mp 172–173 °C. ^{1}H NMR ($CDCl_3$): δ 1.11 (t, 6H, CH_2CH_3), 1.57 (p, 4H, $CH_2CH_2CH_2OH$), 2.23 (s, 6H, pyrr-CH_3), 2.39–2.49 (m, 8H, CH_2CH_3 and $CH_2CH_2CH_2OH$), 3.50 (t, 4H, $CH_2CH_2CH_2OH$), 3.66 (s, 4H, pyrr)$_2$-CH_2), 4.83 (s, 4H, C_6H_5-CH_2), 7.17–7.20 (m, 4H, PhH), 7.25–7.30 (m, 6H, PhH), 8.64 (s, 1H, NH), 9.92 (s, 2H, NH). ^{13}C NMR ($CDCl_3$): δ 11.0, 16.7, 17.7, 20.0, 22.4, 33.2, 62.0, 65.4, 117.2, 119.8, 120.7, 122.2, 127.2, 127.6, 128.3, 133.0, 136.6, 162.1. FAB MS, M^+: *m/e* 693. HR MS, M^+: *m/e* 693.3749 (calcd for $C_{42}H_{51}N_3O_6$, 693.3778).

2,5-Bis[(3-(3-hydroxypropyl)-5-carboxyl-4-methylpyrrol-2-yl)methyl]-3,4-diethylpyrrole (27). 2,5-Bis[(3-(3-hydroxypropyl)-5-((benzyloxy)-carbonyl)-4-methylpyrrol-2-yl)methyl]-3,4-diethylpyrrole (**26**) (15.0 g, 0.02 mol) was placed in a 1-L round-bottom flask and dried *in vacuo* for ca. 30 min. The tripyrrane was dissolved in dry THF (600 mL) with

(21) Sessler, J. L.; Johnson, M. R.; Lynch, V. *J. Org. Chem.* **1987**, *52*, 4394–4397.

(22) Cyr, M. J. Ph.D. Dissertation, University of Texas at Austin, 1991, p 141.

(23) Sessler, J. L.; Mozaffari, A.; Johnson, M. R. *Org. Syn.* **1991**, *70*, 68–78.

triethylamine (10 drops) and 10% Pd on carbon (600 mg), and the reaction was stirred at room temperature under 1 atm of H_2. After 15 h, the suspension was filtered through Celite to remove the catalyst, and the resulting clear solution was concentrated under reduced pressure to yield a light pink solid. This material, obtained in near-quantitative yield, was taken on to the next step without further purification.

2,5-Bis[(5-formyl-3-(3-hydroxypropyl)-4-methylpyrrol-2-yl)methyl]-3,4-diethylpyrrole (28). 2,5-Bis[(3-(3-hydroxypropyl)-5-carboxyl-4-methylpyrrol-2-yl)methyl]-3,4-diethylpyrrole **27** (10 g, 0.02 mol) was placed in a 250-mL round-bottom flask and dried *in vacuo* for ca. 1 h. At room temperature under nitrogen, trifluoroacetic acid (31 mL, 0.40 mol) was added dropwise via syringe. The tripyrrane dissolved with visible evolution of CO_2 to form a homogeneous yellow solution. The reaction was stirred at room temperature for ca. 15 min, then cooled to −20 °C using a dry ice/CCl_4 bath. Freshly distilled triethyl orthoformate (31 mL, 0.20 mol, dried over CaH_2) was added via a syringe to produce a dark orange/yellow solution. This mixture was stirred for an additional 10 min at −20 °C, then the cold bath was removed and 100 mL of distilled water was added dropwise to the solution. The resulting brown suspension was stirred at room temperature for 15 min. The product was collected by filtration, washed several times with water and resuspended into a 50 mL/100 mL/50 mL (H_2O/EtOH/NH_4OH, v/v) mixture. The yellow/brown suspension was stirred for 1 h, filtered, washed several times with water, and then rinsed with a small amount of cold 95% ethanol. At this point, TLC analysis showed a mixture of tripyrranes. Therefore, the crude dialdehyde tripyrrane and $LiOH{\cdot}H_2O$ (2.10 g, 0.05 mol) were added to 400 mL of degassed 95% MeOH, and the suspension was heated to reflux under a N_2 atmosphere. The reaction became homogeneous when heated, and after ca. 1 h, it was slowly cooled to room temperature. The reaction mixture was concentrated under reduced pressure to 75 mL and the resulting slurry placed in the freezer for several hours. The product was filtered and then purified by forming a slurry with 400 mL of methanol and 50 mL of water and heating close to boiling. The suspension was slowly cooled to room temperature, reduced to 150 mL under reduced pressure, and placed in the freezer for several hours. The purified dialdehyde tripyrrane was filtered, rinsed with water and dried *in vacuo* for 24 h to yield 7.65 g (80%) of a light tan powder, mp 164–166 °C. ^{1}H NMR (CD_3OD): δ 0.96 (t, 6H, CH_2CH_3), 1.49 (p, 4H, CH_2CH_2-CH_2OH), 2.25 (s, 6H, pyrr-CH_3), 2.32–2.43 (m, 8H, CH_2CH_3 and CH_2-CH_2CH_2OH), 3.46 (t, 4H, $CH_2CH_2CH_2OH$), 3.85 (s, 4H, $(pyrr)_2$-CH_2), 9.34 (s, 2H, CHO). CI MS, M^+: *m/e* 480. HR MS, M^+: *m/e* 481.2942 (calcd for $C_{28}H_{39}N_3O_4$, 481.2941).

4,5-Diethyl-10,23-dimethyl-9,24-bis(3-hydroxypropyl)-16,17-bis((3-hydroxypropyl)oxy)-13,20,25,26,27-pentaazapentacyclo-[20.2.1.1^{3,6}.1^{8,11}.0^{14,19}]heptacosa-3,5,8,10,12,14,16,18,20,22,24-undecaene (29). 2,5-Bis[(5-formyl-3-(3-hydroxypropyl)-4-methylpyrrol-2-yl)methyl]-3,4-diethylpyrrole (**28**) (1.00 g, 0.002 mol) and 1,2-diamino-4,5-bis((3-hydroxypropyl)oxy)benzene **20** (0.52 g, 0.002 mol) were placed in a 2-L round-bottom flask with 1000 mL of toluene and 200 mL of methanol. The solvents were purged with nitrogen prior to use. Concentrated HCl (0.5 mL) was added and the reaction heated to reflux under nitrogen. The reaction went from a clear suspension of starting materials to a dark red homogeneous solution as the reaction proceeded. After 5 h the reaction was cooled to room temperature and the solvents removed under reduced pressure until the product precipitated out of solution. The remainder of the solvent was decanted off and the macrocycle dried *in vacuo*. The dark red product was recrystallized from methanol/diethylether and yielded 1.4–1.5 g (90–100%), mp 190 °C dec. ^{1}H NMR (CD_3OD): δ 1.11 (t, 6H, CH_2CH_3), 1.76 (p, 4H, pyrr-$CH_2CH_2CH_2OH$), 2.03 (p, 4H, $OCH_2CH_2CH_2OH$), 2.36 (s, 6H, pyrr-CH_3), 2.46 (q, 4H, CH_2CH_3), 2.64 (t, 4H, pyrr-$CH_2CH_2CH_2OH$), 3.61 (t, 4H, pyrr-$CH_2CH_2CH_2OH$), 3.77 (t, 4H, $OCH_2CH_2CH_2OH$), 4.10 (s, 4H, $(pyrr)_2$-CH_2), 4.22 (t, 4H, $OCH_2CH_2CH_2OH$), 7.41 (s, 2H, PhH), 8.30 (s, 2H, HC=N). ^{13}C NMR (CD_3OD): δ 10.0, 17.2, 18.6, 20.9, 24.5, 33.2, 33.5, 59.6, 61.9, 67.8, 107.1, 120.7, 123.8, 125.0, 125.8, 128.7, 144.8, 145.0, 150.7, 154.6. UV/vis (CH_3OH) [λ_{max}, nm]: 365. FAB MS, $(M + H)^+$: *m/e* 703. HRMS, M^+: *m/e* 701.4120 (calcd for $C_{40}H_{55}N_5O_6$: 701.4152). Anal. Calcd $[C_{40}H_{55}N_5O_6](HCl)(CH_3OH)$: C, 63.92; H, 7.85; N, 9.09; Cl, 4.60. Found: C, 64.17; H, 7.68; N, 9.39; Cl, 4.70.

General Procedure for the Synthesis of Water Soluble Lanthanide(III) 4,5-Diethyl-10,23-dimethyl-9,24-bis(3-hydroxypropyl)-16,17-(3-hydroxypropyloxy)-13,20,25,26,27-pentaazapentacyclo[20.2.1.1^{3,6}.1^{8,11}.0^{14,19}]-heptacosa-1,3,5,7,9,11(27),12,14,16,18,20,22(25),23-tridecaene (30). One equivalent of the hydrochloride salt of the macrocycle 4,5-diethyl-10,-23-dimethyl-9,24-bis(3-hydroxypropyl)-16,17-bis(3-hydroxypropyloxy)-13,20,25,26,27-pentaazapentacyclo[20.2.1.1^{3,6}.1^{8,11}.0^{14,19}]heptacosa-3,5,8,10,12,14,16,18,20,22,24-undecaene (**29**), 1.5 equiv of the $Ln(NO_3)_3{\cdot}xH_2O$ metal salt, 2–3 equiv of tetrabutylammonium nitrate ((TBA)-NO_3), and triethylamine (ca. 1 mL) were mixed together in methanol and heated to reflux under air. After completion of the reaction (as judged by the UV/vis spectrum of the reaction mixture), the deep green solution was cooled to room temperature, the solvent removed under reduced pressure, and the crude complex dried *in vacuo* for several hours. A solution of dichloromethane/methanol (99:1 v/v) was added to the crude complex and the suspension was sonicated for a few minutes. The green suspension was filtered in order to remove red/brown impurities in the filtrate (incomplete oxidation products) and excess triethylamine. The resulting deep green solid was first dissolved in methanol and then chloroform was added to reduce the polarity of the mixture (1:2 v/v). This solution was filtered through celite and loaded on a (pretreated/prewashed 1 M $NaNO_3$) neutral alumina column (10 cm). The column was first eluted with a 1:10 (v/v) methanol/chloroform solution by gravity to remove a reddish brown impurity. The metal complex was then obtained by eluting the column with chloroform containing increasing amounts of methanol (20–50%). The purified lanthanide(III) texaphyrin complex was recrystallized by dissolving the complex in methanol/chloroform and carefully layering the dark green solution with a small amount of methanol, then with diethylether. The layered solution was kept at room temperature in the dark for a few days. Some of the lanthanide(III) texaphyrin complexes formed single crystals by this method. Other complexes were recrystallized twice for analytically pure measurements and characterizations.

Lanthanum(III) Complex 31. The hydrochloride salt of macrocycle **29** (300 mg, 0.407 mmol), $La(NO_3)_3{\cdot}6H_2O$ (350 mg, 0.814 mmol), (TBA)-NO_3 (305 mg, 1.0 mmol), and triethylamine (ca. 0.5 mL) in 350 mL of methanol were heated to reflux under air for 10 h. After workup using the general procedure outlined above, 132 mg of the complex was obtained (34%). ^{1}H NMR (CD_3OD): δ 1.68 (t, 6H, CH_2CH_3), 2.22–2.30 (m, 4H, pyrr-$CH_2CH_2CH_2OH$, and 4H, $OCH_2CH_2CH_2OH$), 3.20 (s, 6H, pyrr-CH_3), 3.72–3.78 (m, 4H, CH_2CH_3 and 4H, pyrr-$CH_2CH_2CH_2OH$, and 4H, pyrr-$CH_2CH_2CH_2OH$), 3.94 (t, 4H, $OCH_2CH_2CH_2OH$), 4.78 (m, 4H, $OCH_2CH_2CH_2OH$), 9.37 (s, 2H, ArH), 9.87 (s, 2H, $(pyrr)_2C{=}CH$), 11.71 (s, 2H, HC=N). ^{13}C NMR (CD_3OD): δ 11.0, 18.9, 20.3, 23.0, 33.3, 36.3, 59.7, 62.2, 68.1, 101.5, 118.5, 137.1, 140.3, 144.6, 147.5, 148.2, 152.9, 154.9, 159.4. UV/vis [(MeOH) λ_{max}, nm (log ϵ)]: 355 (4.34), 417 (4.73), 476 (5.06), 685.5 (4.08), 746 (4.59). FAB MS, M^+: *m/e* 835. HRMS, $(M + H)^+$: *m/e* 836.2919 (calcd for $C_{40}H_{51}N_5O_6{}^{139}La$, 836.2903). Anal. Calcd for $[C_{40}H_{50}N_5O_6La](NO_3)_2(H_2O)_2$: C, 48.23; H, 5.47; N, 9.85. Found: C, 47.93; H, 5.41; N, 9.77.

Cerium(III) Complex 32. The hydrochloride salt of macrocycle **29** (300 mg, 0.407 mmol), $Ce(NO_3)_3{\cdot}6H_2O$ (265 mg, 0.611 mmol), (TBA)-NO_3 (305 mg, 1.0 mmol) and triethylamine (ca. 0.5 mL) in 350 mL of methanol were heated to reflux under air for 7 h. It is important to note that initially the reaction mixture formed a suspension; however, as the product formed, the solution became homogeneous. After workup using the general procedure outlined above, 143 mg of dark green crystals were obtained (37%). This material was suitable for X-ray diffraction analysis. UV/vis [(MeOH) λ_{max}, nm (log ϵ)]: 349.5 (4.34), 416.5 (4.70), 476.5 (5.05), 684 (4.07), 741 (4.56). FAB MS, M^+: *m/e* 836. HRMS, $(M + H)^+$: *m/e* 836.2807 (calcd for $C_{40}H_{51}N_5O_6{}^{140}Ce$, 836.2816). Anal. Calcd for $[C_{40}H_{50}N_5O_6Ce](NO_3)_2(H_2O)_3$: C, 47.32; H, 5.56; N, 9.66. Found: C, 46.98; H, 5.22; N, 9.63.

Praseodymium(III) Complex 33. The hydrochloride salt of macrocycle **29** (300 mg, 0.407 mmol), $Pr(NO_3)_3{\cdot}5H_2O$ (255 mg, 0.611 mmol), (TBA)-NO_3 (305 mg, 1.0 mmol), and triethylamine (ca. 0.5 mL) in 350 mL of methanol were heated to reflux under air for 10 h. After workup using the general procedure outlined above, 200 mg of the complex was obtained (51%). UV/vis [(MeOH) λ_{max}, nm (log ϵ)]: 352 (4.32), 416.5 (4.69), 476.5 (5.04), 689 (4.07), 744.5 (4.57). FAB MS, M^+: *m/e* 838. HRMS, M^+: *m/e* 837.2823 (calcd for $C_{40}H_{50}N_5O_6{}^{141}Pr$, 837.2838). Anal. Calcd for $[C_{40}H_{50}N_5O_6Pr](NO_3)_2(CH_3OH)(H_2O)$: C, 48.65; H, 5.58; N, 9.69. Found: C, 48.75; H, 5.52; N, 9.71.

Neodymium(III) Complex 34. The hydrochloride salt macrocycle **29** (300 mg, 0.407 mmol), $Nd(NO_3)_3{\cdot}6H_2O$ (267 mg, 0.611 mmol), (TBA)-NO_3 (305 mg, 1.0 mmol), and triethylamine (ca. 0.5 mL) in 350 mL of methanol were heated to reflux under air for 12 h. After workup using the general procedure outlined above, 125 mg of the complex was obtained (32%). UV/vis [(MeOH) λ_{max}, nm (log ϵ)]: 353.5 (4.32), 416 (4.68), 476 (5.05), 688 (4.06), 742.5 (4.56). FAB MS, M^+: *m/e* 839. HRMS, M^+: *m/e* 838.2828 (calcd for $C_{40}H_{50}N_5O_6{}^{142}Nd$, 838.2838). Anal. Calcd for $[C_{40}H_{50}N_5O_6Nd](NO_3)_2(CH_3OH)$: C, 49.48; H, 5.47; N, 9.86. Found: C, 49.23; H, 5.49; N, 9.83.

Samarium(III) Complex 35. The hydrochloride salt of macrocycle **29** (300 mg, 0.407 mmol), $Sm(NO_3)_3 \cdot 5H_2O$ (270 mg, 0.611 mmol), (TBA)NO_3 (305 mg, 1.0 mmol), and triethylamine (ca. 0.5 mL) in 350 mL of methanol were heated to reflux under air for 7 h. After workup using the general procedure outlined above, 183 mg of a dark green crystalline solid was obtained (46%). This material has the potential for X-ray diffraction. UV/vis [(MeOH) λ_{max}, nm (log ϵ)]: 354.5 (4.36), 415.5 (4.71), 475.5 (5.09), 682 (4.09), 741 (4.61). FAB MS, M^+: *m/e* 849. HRMS, M^+: *m/e* 848.2957 (calcd for $C_{40}H_{50}N_5O_6{}^{152}Sm$, 848.2959). Anal. Calcd for $[C_{40}H_{50}N_5O_6Sm](NO_3)_2(CH_3OH)$: C, 48.99; H, 5.42; N, 9.76. Found: C, 48.79; H, 5.64; N, 9.43.

Europium(III) Complex 36. The hydrochloride salt of macrocycle **29** (400 mg, 0.543 mmol), $Eu(NO_3)_3 \cdot 5H_2O$ (290 mg, 0.65 mmol), (TBA)NO_3 (500 mg, 1.64 mmol) and triethylamine (ca. 1 mL) in 350 mL of methanol were heated to reflux under air for 16 h. After working using the general procedure outlined above, 255 mg of a dark green crystalline solid was obtained (48%). This material was suitable for X-ray diffraction analysis. UV/vis [(MeOH) λ_{max}, nm (log ϵ)]: 414 (4.72), 475.5 (5.10), 678 (4.08), 739.5 (4.63). FAB MS, $(M + H)^+$: *m/e* 850; HRMS, M^+: *m/e* 849.2961 (calcd for $C_{40}H_{50}N_5O_6{}^{153}Eu$, 849.2974). Anal. Calcd for $[C_{40}H_{50}N_5O_6Eu](NO_3)_2(H_2O)$: C, 47.56; H, 5.39; N, 9.71. Found: C, 47.47; H, 5.45; N, 9.64.

Gadolinium(III) Complex 37. The hydrochloride salt of macrocycle **29** (750 mg, 1 mmol), $Gd(NO_3)_3 \cdot 5H_2O$ (660 mg, 1.5 mmol), (TBA)NO_3 (930 mg, 3.0 mmol), and triethylamine (ca. 1 mL) in 600 mL of methanol were heated to reflux under air for 12 h. After workup using the procedure outlined above, the dark green complex was recrystallized from chloroform/methanol/diethyl ether to yield 700 mg (72%) of a deep green crystalline solid. X-ray quality single crystals were obtained by dissolving the complex in methanol/chloroform and carefully layering the dark green solution with a small amount of methanol, then with diethyl ether. The layered solution was kept at room temperature in the dark for a few days. UV/vis [(MeOH) λ_{max}, nm (log ϵ)]: 358 (4.33), 416 (4.72), 478 (5.12), 678 (4.03), 737.5 (4.64); [(H_2O) λ_{max}, nm (log ϵ)]: 347 (4.43), 419 (4.75), 469 (5.08), 740 (4.60). IR (KBr, cm^{-1}, major peaks): ν 3299 (OH), 1647 (C=N), 1601 (C=N), 1507, 1456, 1437, 1385 (NO_3^-), 1290, 1221, 1098, 1082. FAB MS, M^+: *m/e* 854. HRMS, M^+: *m/e* 854.2989 (calcd for $C_{40}H_{50}N_5O_6{}^{158}Gd$, 854.300. Anal. Calcd for $[C_{40}H_{50}N_5O_6Gd](NO_3)_2(CH_3OH)(H_2O)$: C, 47.85; H, 5.49; N, 9.53. Found: C, 47.62; H, 5.37; N, 9.54.

Note: If the alumina is not pretreated with a $NaNO_3$ wash, the Gd(III) will not have two nitrate counter anions, instead it will have one nitrate and one chloride counter anion: Anal. Calcd for $[C_{40}H_{50}N_5O_6Gd](NO_3)Cl(H_2O)_2$: C, 48.65; H, 5.51; N, 8.51; Cl, 3.59. Found: C, 48.21; H, 5.58; N, 8.34; Cl, 3.62.

Terbium(III) Complex 38. The hydrochloride salt of macrocycle **29** (300 mg, 0.407 mmol), $Tb(NO_3)_3 \cdot 6H_2O$ (276 mg, 0.611 mmol), (TBA)NO_3 (305 mg, 1.64 mmol) and triethylamine (ca. 0.5 mL) in 350 mL of methanol were heated to reflux under air for 12 h. After workup using the general procedure outlined above, 152 mg of the complex was obtained (38%). UV/vis [(MeOH) λ_{max}, nm (log ϵ)]: 353 (4.35), 414 (4.71), 474.5 (5.09), 680 (4.08), 737 (4.62); FAB MS, M^+: *m/e* 856. HRMS, M^+: *m/e* 855.3017 (calcd for $C_{40}H_{50}N_5O_6{}^{159}Tb$, 855.3015). Anal. Calcd for $[C_{40}H_{50}N_5O_6Tb](NO_3)_2(CH_3OH)(H_2O)$: C, 47.80; H, 5.48; N, 9.52. Found: C, 48.11; H, 5.28; N, 9.75.

Dysprosium(III) Complex 39. The hydrochloride salt of macrocycle **29** (300 mg, 0.407 mmol), $Dy(NO_3)_3 \cdot 5H_2O$ (266 mg, 0.611 mmol), (TBA)NO_3 (305 mg, 1.64 mmol), and triethylamine (ca. 0.5 mL) in 350 mL of methanol were heated to reflux under air for 5 h. After workup using the general procedure outlined above, 250 mg of the complex was obtained (62%). UV/vis [(MeOH) λ_{max}, nm (log ϵ)]: 354 (4.32), 414 (4.68), 475 (5.07), 677.5 (4.03), 735.5 (4.60). FAB MS, $(M + H)^+$: *m/e* 861. HRMS, M^+: *m/e* 860.3048 (calcd. for $C_{40}H_{50}N_5O_6{}^{164}Dy$, 860.3053). Anal. Calcd for $[C_{40}H_{50}N_5O_6Dy](NO_3)_2(H_2O)$: C, 47.89; H, 5.23; N, 9.78. Found: C, 47.97; H, 5.22; N, 9.72.

Holmium(III) Complex 40. The hydrochloride salt of macrocycle **29** (300 mg, 0.407 mmol), $Ho(NO_3)_3 \cdot 5H_2O$ (269 mg, 0.611 mmol), (TBA)NO_3 (305 mg, 1.64 mmol), and triethylamine (ca. 0.5 mL) in 350 mL of methanol were heated to reflux under air for 12 h. After workup using the general procedure outlined above, 220 mg of the complex was obtained (55%). UV/vis [(MeOH) λ_{max}, nm (log ϵ)]: 354 (4.35), 414 (4.72), 475.5 (5.12), 677 (4.08), 734 (4.65). FAB MS, M^+: *m/e* 862. HRMS, M^+: *m/e* 861.3044 (calcd for $C_{40}H_{50}N_5O_6{}^{165}Ho$, 861.3064). Anal. Calcd for $[C_{40}H_{50}N_5O_6Ho](NO_3)_2(CH_3OH)(H_2O)$: C, 47.52; H, 5.45; N, 9.47. Found: C, 47.55; H, 5.26; N, 9.30.

Erbium(III) Complex 41. The hydrochloride salt of macrocycle **29** (300 mg, 0.407 mmol), $Er(NO_3)_3 \cdot 5H_2O$ (270 mg, 0.611 mmol), (TBA)NO_3 (305 mg, 1.64 mmol), and triethylamine (ca. 0.5 mL) in 350 mL of methanol were heated to reflux under air for 12 h. After workup using the general procedure outlined above, 143 mg of the complex was obtained (36%). UV/vis [(MeOH) λ_{max}, nm (log ϵ)]: 355.5 (4.36), 414.5 (4.72), 477 (5.13), 672 (4.08), 732 (4.66). FAB MS, M^+: *m/e* 863. HRMS, M^+: *m/e* 865.3110 (calcd for $C_{40}H_{50}N_5O_6{}^{166}Er$, 862.3064). Anal. Calcd for $[C_{40}H_{50}N_5O_6Er](NO_3)_2(CH_3OH)$: C, 48.32; H, 5.34; N, 9.63. Found: C, 48.14; H, 5.14; N, 9.55.

Thulium(III) Complex 42. The hydrochloride salt of macrocycle **29** (300 mg, 0.407 mmol), $Tm(NO_3)_3 \cdot 5H_2O$ (274 mg, 0.611 mmol), (TBA)NO_3 (305 mg, 1.64 mmol), and triethylamine (ca. 0.5 mL) in 350 mL of methanol were heated to reflux under air for 22 h. After workup using the general procedure outlined above, 150 mg of the complex was obtained (37%). This complex is more difficult to purify due to its lower solubility in methanol/chloroform solutions, which leads to its lower yield. UV/vis [(MeOH) λ_{max}, nm (log ϵ)]: 355.5 (4.36), 414.5 (4.72), 477 (5.13), 672 (4.08), 732 (4.66). FAB MS, M^+: *m/e* 866. HRMS, M^+: *m/e* 865.3110 (calcd for $C_{40}H_{50}N_5O_6{}^{169}Tm$, 865.3103). Anal. Calcd for $[C_{40}H_{50}N_5O_6Tm](NO_3)_2(H_2O)_2$: C, 46.82; H, 5.31; N, 9.56. Found: C, 46.85; H, 5.23; N, 9.38.

Ytterbium(III) Complex 43. The hydrochloride salt of macrocycle **29** (300 mg, 0.407 mmol), $Yb(NO_3)_3 \cdot 5H_2O$ (274 mg, 0.611 mmol), (TBA)NO_3 (305 mg, 1.64 mmol), and triethylamine (ca. 0.5 mL) in 350 mL of methanol were heated to reflux under air for 24 h. After work up using the general procedure outlined above, 220 mg of the complex was obtained (54%). FAB MS, M^+: *m/e* 870. HRMS, M^+: *m/e* 870.3132 (calcd for $C_{40}H_{50}N_5O_6{}^{174}Yb$, 870.3149).

Lutetium(III) Complex 44. The hydrochloride salt of macrocycle **29** (300 mg, 0.407 mmol), $Lu(NO_3)_3 \cdot H_2O$ (220 mg, 0.611 mmol), (TBA)NO_3 (305 mg, 1.64 mmol), and triethylamine (ca. 0.5 mL) in 350 mL methanol were heated to reflux under air for 24 h. After workup using the general procedure outlined above, 150 mg of the complex was obtained (37%). This complex has very low solubility in methanol/chloroform solution. Almost half of the product remained on the column during purification. FAB MS, M^+: *m/e* 872. HRMS, M^+: *m/e* 871.3154 (calcd for $C_{40}H_{50}N_5O_6{}^{175}Lu$, 871.3169).

X-ray Crystallography. Crystals were grown from a solution of the appropriate complex in $CHCl_3/CH_3OH$ layered with diethyl ether. The crystals, to varying degrees, decomposed upon removal from the mother liquor. Crystals were stabilized for short periods by placement in mineral oil where suitable crystals could be selected and rapidly mounted on the diffractometer. At the temperature of data collection (≤–90 °C), the crystals remained stable indefinitely. Details of the crystal data, data collection, and refinement are listed in Table I. Data reduction and decay correction were performed using the SHELXTL-*Plus* software package.[24] The structure was solved by direct methods and refined by full-matrix least-squares[24] with anisotropic thermal parameters for most of the non-H atoms. Most H atom positions were idealized (C–H = 0.96 Å) with U_{iso} fixed at $1.2U_{eq}$ of the relevant C atom. Whenever possible O–H hydrogen atom positions were obtained from a ΔF map but were subsequently refined tied to their respective O atom with U_{iso} set to $1.2U_{eq}$ except for **36** where the O–H hydrogens were refined without constraints. Where OH hydrogen positions could not be obtained, they were not calculated. Due to the large number of parameters, the structures were all refined in blocks. Absorption corrections were applied on the basis of measured crystal faces except for **37**. For **37**, which was especially sensitive to loss of solvent when removed from the mother liquor and had to be mounted in stopcock grease, accurate face measurements could not be made. The absorption correction program XABS[24] was therefore used. The function, $\sum w(|F_o| - |F_c|)^2$, was minimized, where $w = 1/(\sigma(F_o))^2$ and $\sigma(F_o) = \{0.5kI^{-1/2}[(\sigma(I))^2 + (0.02I)^2]^{1/2}\}$. The intensity, I, is given by $(I_{peak} - I_{background})$(scan rate); where 0.02 is a factor to downweight intense reflections and to account for instrument instability and k is the correction due to Lp effects, absorption, and decay. $\sigma(I)$ was estimated from counting statistics; $\sigma(I) = [(I_{peak} + I_{background})^{1/2}$(scan rate)]. Neutral atom scattering factors for the non-H atoms were taken from Cromer and Mann,[25] with the anomalous-dispersion corrections taken from the work of Cromer and Liberman.[26] The scattering factors for the H atoms were obtained from Stewart, Davidson, and Simpson.[27]

(24) Sheldrick, G. M.; *SHELXTL-Plus* (Version 4.11); Siemens X-ray Analytical Instruments, Inc.: Madison, WI, 1991.
(25) Cromer, D. T.; Mann, J. B. *Acta Crystallogr.* **1968**, *A24*, 321–324.
(26) Cromer, D. T.; Liberman, D. *J. Chem. Phys.* **1970**, *53*, 1891–1898.
(27) Stewart, R. F.; Davidson, E. R.; Simpson, W. T. *J. Phys. Chem.* **1965**, *42*, 3175–3187.

Table I. Crystallographic Data for Lanthanide(III) Texaphyrin Complexes[a]

	3	9	22	36	37
formula	$C_{35}H_{42}N_7O_9La$	$C_{34}H_{38}N_7O_8Gd$	$C_{39}H_{50}N_7O_{12}Lu$	$C_{44}H_{60}N_7O_{16}Eu$	$C_{44}H_{60}N_7O_{16}Gd$
fw	834.66	807.04	983.83	1094.96	1100.24
a, Å	10.716(3)	10.794(3)	9.070(2)	11.4510(14)	11.450(3)
b, Å	10.738(2)	10.940(3)	10.334(3)	14.652(2)	14.641(4)
c, Å	18.688(3)	18.729(5)	24.459(7)	16.568(4)	16.566(6)
α, deg	78.57(1)	83.63(2)	78.06(2)	104.210(15)	104.17(2)
β, deg	83.00(2)	81.67(2)	79.45(3)	103.497(15)	103.50(2)
γ, deg	60.11(1)	60.06(2)	68.64(2)	104.428(10)	104.31(2)
V, Å^3	2478.1(14)	3751(2)	2088.0(9)	2537.7(7)	2478.0(14)
Z	2	2	2	2	2
cryst syst	triclinic	triclinic	triclinic	triclinic	triclinic
space group	$P\bar{1}$ (No. 2)	$P\bar{1}$ (No. 2)	$P\bar{1}$ (No. 2)	$P\bar{1}$ (No. 2)	$P\bar{1}$ (No. 2)
T, °C	−90	−100	−90	−90	−90
radiation	graphite monochromatized, Mo Kα (λ ξ 0.7107 Å)				
2θ range, deg	4–55	4–50	4–50	4–60	4–55
scan speed, (deg/min)	3–6	3–6	3–6	3–6	3–6
scan range (ω scan), deg	1.2	1.2	1.2	1.0	1.2
ρ_{calc}, g/cm^3	1.53	1.41	1.56	1.43	1.47
no. of reflcns measd	8854	11403	8513	17413	12523
no. of unique reflns	8403	6608	7352	14443	11383
R_{int}	0.018	0.02	0.014	0.013	0.0194
μ, cm^{-1}	12.33	18.04	24.33	13.05	14.143
transm factor[b] range	0.6474–0.9377	0.5252–0.8522	0.5663–0.8413	0.569–0.7985	0.79–2.37
cryst size, mm	0.05 × 0.4 × 0.6	0.1 × 0.16 × 0.52	0.07 × 0.3 × 0.3	0.17 × 0.44 × 0.55	0.11 × 0.29 × 0.7
no. of reflcns used	6234	5558	6175	11823	9104
no. of reflcns rejected	2169	1050	1177	2620	2279
rejection criterion	[$F < 6(\sigma(F))$]	[$F < 6(\sigma(F))$]	[$F < 6(\sigma(F))$]	[$F < 6(\sigma(F))$]	[$F < 4(\sigma(F))$]
$R(F)$[c]	0.0412	0.0373	0.0293	0.0320	0.0477
$R_w(F)$	0.0447	0.0457	0.0353	0.0400	0.0479
goodness of fit	1.253	1.566	1.209	1.340	1.342
no. of params	469	477	536	633	613
max $\lvert\Delta/\sigma\rvert$	<0.1	<0.1	<0.1	<0.1	<0.1
min, max peaks, e/Å^3	−0.78, 1.06	−0.99, 1.88	−0.53, 0.84	−0.70, 1.47	−1.79, 2.68

[a] Data for all samples were collected on a Nicolet P3 diffractometer using a Nicolet LT-2-low-temperature delivery system. Lattice parameters were obtained from the least-squares refinement of 45 reflections with 13.9 < 2θ < 23.0° for **3**, 40 reflections with 15.8 < 2θ < 22.0° for **9**, 40 reflections with 15.4 < 2θ < 20.0° for **22**, 50 reflections with 19.7 < 2θ < 24.9.0° for **36**, and 43 reflections with 16.5 < 2θ < 22.6° for **37**. [b] Absorption correction was based on measured crystal faces for **3**, **9**, **22** and **36**. For **37**, Hoppe's empirical absorption correction method was used (see Experimental Section). [c] The function, $\sum w(|F_o| - |F_c|)^2$, was minimized where $w = 1/(\sigma(F_o)^2 + (0.02F)^2)$.

Values used to calculate the linear absorption coefficient are from ref 28. All figures were generated using SHELXTL-*Plus*.[24] Other computer programs used in this work are listed elsewhere.[29]

For **9**, an unusual disorder exists in the coordination sphere of Gd. Both 9- and 10-coordinate Gd are observed. The 10-coordinate species is similar to **3** with two bidentate NO_3^- anions above the texaphyrin core and a coordinated CH_3OH below (cf. Figure 3). The 9-coordinate Gd species is similar to **36** and **37** having one bidentate NO_3^- (N1B, O1B, O2B, O3B) and one CH_3OH (O1D, C2D) above the texaphyrin core and one CH_3OH below (cf. Figure 3). The disorder is such that when the CH_3OH is coordinated, a noncoordinated NO_3^- group is within H-bonding distance to it. When the NO_3^- is coordinated, an O atom, O1W, is within H-bonding distance to the NO_3^-. The disorder is 50–50 as determined by refining the site-occupancy factors of the coordinated and noncoordinated NO_3^- ions. The assignment of the atom, O1W, as a water molecule was made because no second peak with an appreciable electron density could be found in the ΔF maps. However, in this region, many small peaks (all less than 0.5 e/Å^3) were observed and given the disorder, the second carbon peak may well have been obscured.

For **22**, a mixture of methanol and ethanol coordination to Lu(III) below the N_5 plane is observed. After **22** was refined with methanol coordination, a peak of 1.5 e/Å^3 was observed within bonding distance to C1C. This peak was assumed to be due to a small amount of ethanol impurity. (Ethanol is present as a stabilizer in the chloroform used in our labs.) This atom, C2C, was refined isotropically. Its occupancy factor was estimated at 34% by fixing its U_{iso} at 1.2U_{eq} of C1C and refining the site-occupancy factor. Thereafter, the site-occupancy factor was fixed and U_{iso} was refined.

Results and Discussion

Lanthanide(III) Dimethoxytexaphyrins. Synthesis. With the nonaromatic ligand **45**[19] in hand, we set out to prepare well-characterized lanthanide(III) texaphyrin complexes. During the course of this work, we were able to optimize the original oxidation and metallation reaction reported earlier[16,17,19] by heating **45** in presence of $Ln(NO_3)_3 \cdot xH_2O$ and triethylamine in oxygenated methanol. Yields of the purified metal complexes improved from ca. 25% using the original preparation[16,17] to ca. 55–70% for all of the heavier lanthanide texaphyrin complexes (Nd–Lu, except Pm). The lighter lanthanide cations (La–Pr) produced slightly lower yields of complex (ca. 30%). All of these Ln(III) complexes (**3–16**) were formulated as 1:1, metal-ligand complexes as characterized by mass spectrometry and microanalytical data. In addition, the La(III) **3** and Gd(III) **9** complexes were characterized by X-ray crystallography (see below). All of the complexes **3–16** exhibited characteristic UV/vis spectra, with the Soret-like and Q-type bands in the 473- and 728–743-nm regions, respectively (cf. Experimental Section). In all cases, these spectra were thus very similar to the already published spectrum of the gadolinium(III) texaphyrin complex **1**.[17] Furthermore, the ^{1}H NMR of the diamagnetic lanthanum(III) complex **3** shows general features[16] which are typical of other analogous aromatic expanded porphyrins,[15] such as, sapphyrin,[30] pentaphyrin,[31] rubyrin,[32] and hexaphyrin.[33] In particular, as would be expected in the presence of a strong diamagnetic ring current, the imine (δ = 11.43 ppm) and aromatic (δ = 9.02 ppm) peaks are shifted to lower field. Also, the bridged methylene signals of **45** (at δ = 3.91 ppm[19]) are replaced in **3** by a sharp singlet, at 9.58 ppm, ascribable to the bridging "meso" protons. These findings are in accord with earlier studies[16] in the texaphyrin series.

The Gd(III) complexes **1**[17] and **9** were somewhat soluble in 3:1 mixtures of water/methanol (a 10^{-5} M solution could be formed in 75% water/methanol). However, these complexes proved to be insufficiently soluble in pure water to allow their use as *in vivo*

(28) *International Tables for X-ray Crystallography*, Kynoch Press: Birmingham, England, 1974; Vol. IV, p 55.
(29) Gadol, S. M.; Davis, R. E. *Organometallics* **1982**, *1*, 1607–1613.

Scheme I

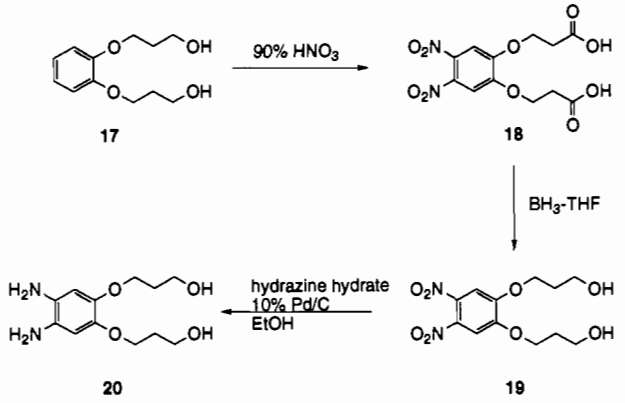

paramagnetic contrast agents. Therefore, we proceeded to synthesize a gadolinium(III) texaphyrin derivative that would be soluble at concentrations required for MR imaging (1–0.1 mM). Since complexes **1** and **9** were soluble in methanol containing high concentrations of water, we envisioned that modifying **1** or **9**, by appending several hydroxyl substituents around the periphery of the macrocycle, would produce a complex (e.g., **21** or **30**) that would be water soluble.[30]

Our first approach was to modify the diamine portion of the macrocycle, as summarized in Scheme I. Here, nitration of *o*-bis-((3-hydroxypropyl)oxy)benzene **17**[20] was used to produce the dinitro diacid intermediate **18** in 55% yield. Subsequent reduction of the carboxylate **18** with borane–THF gave **19** in 90% yield. This was then followed by reduction of the dinitro functionality to afford the desired diamine **20** in 91% yield. Subsequent acid-catalyzed condensation between 2,5-bis((3-ethyl-5-formyl-4-methylpyrrol-2-yl)methyl)-3,4-diethylpyrrole[21] and **20** then produced the key nonaromatic texaphyrin-type ligand **46** in quantitative yield. Final oxidative metallation carried out in the presence of $Lu(NO_3)_3 \cdot H_2O$ then produced the dihydroxy-substituted Lu(III) complex **22** in ca. 37%. Unfortunately, this complex proved *organic soluble* not water soluble. In fact, X-ray quality single crystals of this material were obtained by recrystallizing from a mixture of chloroform, methanol, and diethyl ether.

Due to the low water solubility of the Lu(III) complex **22** and its analogues, we sought to prepare a tetrahydroxylated texaphyrin such as that represented by the generalized formula **30**. As detailed below, this approach has in fact proved successful in terms of achieving the sought for water solubility. The critical intermediate required for the synthesis of **30** is the tripyrrane dialdehyde **28**. Its synthesis is summarized in Scheme II. Here, the condensation of 2 equiv of 2-(acetoxymethyl)-5-((benzyloxy)-carbonyl)-4-methyl-3-((methoxycarbonyl)ethyl)pyrrole (**23**)[22] with 3,4-diethylpyrrole (**24**)[23] by acid catalysis was used to produce the bis(methyl ester)-functionalized tripyrrane **25** in 75% yield. The methyl esters were then reduced to hydroxy substituents (compound **26**) using borane–THF in 85% yield. Although this effects the required transformations, the benzyl esters in the α-position remain intact. At this point, debenzylation of **27**, followed by subsequent Clezy formylation[21] of the intermediate diacid tripyrrane **27** and basic hydrolysis with LiOH, provides

Scheme II

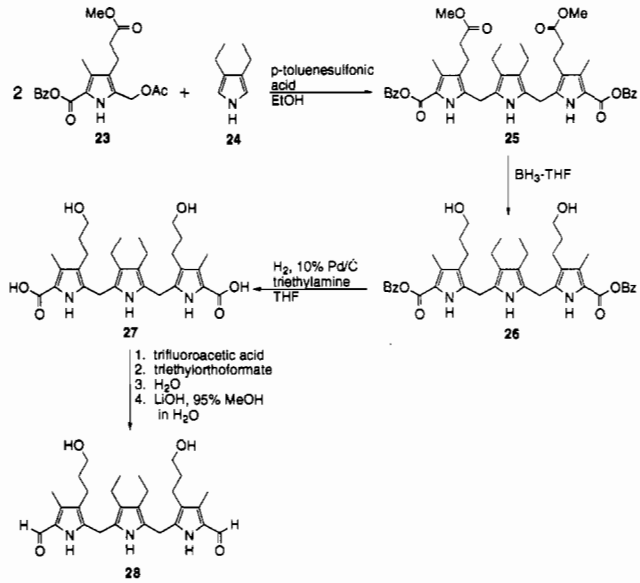

the tripyrrane dialdehyde **28** in an 80% overall yield. The basic hydrolysis, although, not required for Clezy formylation, appears necessary to cleave various mono- and di-TFA ester side products formed during the decarboxylation formylation sequence.

Acid-catalyzed Schiff-base condensation[19,21] between **20** and **28** produced the so-called "sp^3" nonaromatic macrocycle **29** in quantitative yield (Scheme III). Macrocycle **29** is quite stable, decomposing only slightly over a period of months when stored in a freezer. Oxidation and metalation of **29** in the presence of 1.5 equiv of lanthanide(III) metal salt, triethylamine, and air in boiling methanol produces a deep green metal complex within 3–24 h (as judged by UV/vis). All the lanthanide(III) [La–Lu, except Pm] texaphyrin complexes **31–44** were isolated with unoptimized yields ranging from 34% to 75%. Satisfactory spectroscopic and mass spectrometric data were obtained for all new compounds. Single crystals suitable for X-ray diffraction analysis of the Eu(III) and Gd(III) complexes **36** and **37** (see Figure 2), respectively, were obtained by dissolving each complex in $MeOH/CHCl_3$ and layering with diethyl ether.

In addition to providing crystalline material in the case of certain complexes, the choice of four peripheral hydroxyl groups also solved the critical problem of solubility. All of the complexes **31–44** proved to be water soluble to a greater or lesser degree. In the case of the Gd(III) complex **37**, which has been the most extensively studied, the solubility was found to be ca. 2 mg/mL in pure water and up to 8 mg/mL in 5% aqueous dextrose solution. A similar level of solubility was also encountered for analogous complexes of the lighter lanthanide(III) cations. However, the solubility in water was found to be remarkably reduced in the case of the heavier congeners with the Lu(III) complex **44** being only sparingly soluble in the absence of some added cosolvent such as MeOH or DMSO. Nonetheless, the success achieved in the case of **37** (as well as **31–36**) serves to highlight that the use of hydroxyl groups as water-solubilizing substituents is an ostensibly viable one.

Structural Features. During the course of the preparation of several lanthanide(III) texaphyrin complexes, we were able to isolate X-ray quality crystals and elucidate the solid-state structure of the La(III) complex **3**, the Eu(III) complex **36**, the Gd(III) complexes **9** and **37**, and the Lu(III) complex **22** (see Figures 1–4 and Tables I and II). These structures exhibit several distinctive features. They differ from one another slightly in relation to coordination number and distortion of the macrocyclic ligand framework. Nonetheless, in many respects, these structures resemble each other quite closely. Thus, taken together, they serve to define several interesting trends relating both to lanthanide

(30) (a) Bauer, V. J.; Clive, D. L.; Dolphin, D.; Paine, J. B., III; Harris, F. L.; King, M. M.; Loder, H.; Wang, S.-W. C.; Woodward, R. B. *J. Am. Chem. Soc.* **1983**, *105*, 6429–6436. (b) Broadhurst, M. J.; Grigg, R.; Johnson, A. W. *J. Chem. Soc., Perkin Trans. 1*, **1972**, 2111–2116. (c) Sessler, J. L.; Cyr, M. J.; Lynch, V.; McGhee, E.; Ibers, J. A. *J. Am. Chem. Soc.* **1990**, *112*, 2810–2813. (d) Sessler, J. L.; Cyr, M. J.; Burrell, A. K. *Synlett* **1991**, 127–133.

(31) (a) Rexhausen, H.; Gossauer, A. *J. Chem. Soc., Chem. Commun.* **1983**, 275. (b) Burrell, A. K.; Hemmi, G.; Lynch, V.; Sessler, J. L. *J. Am. Chem. Soc.* **1991**, *113*, 4690–4692.

(32) Sessler, J. L.; Morishima, T.; Lynch, V. *Angew. Chem., Int. Ed. Engl.* **1991**, *30*, 977–980.

(33) Gossauer, A. *Bull. Soc. Chim. Belg.* **1983**, *92*, 793–795.

Scheme III

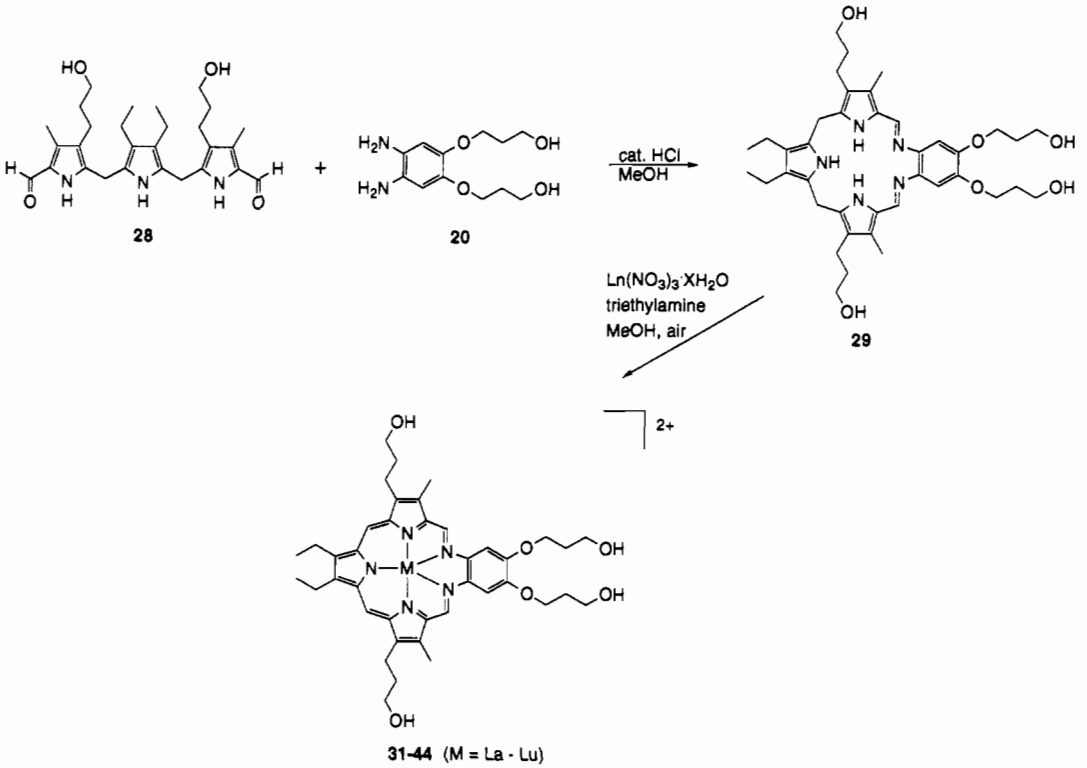

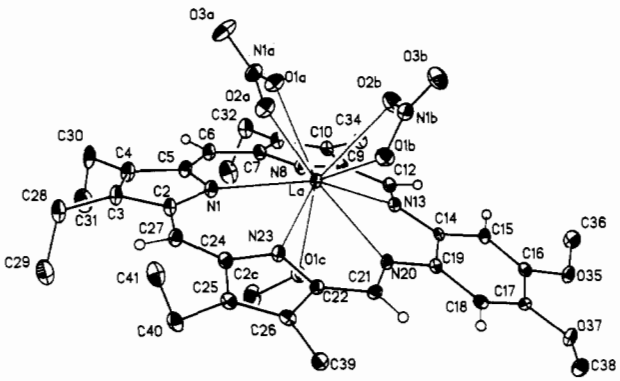

Figure 1. View of lanthanide(III) texaphyrin **3** showing the representative labeling scheme for the macrocycle. Thermal ellipsoids are scaled to the 30% probability level. Most hydrogen atoms are omitted for clarity. Labels for pyrollic carbon, C11, and ethylenic methyl carbon, C33, were omitted for clarity. See Table II for the pertinent geometric parameters.

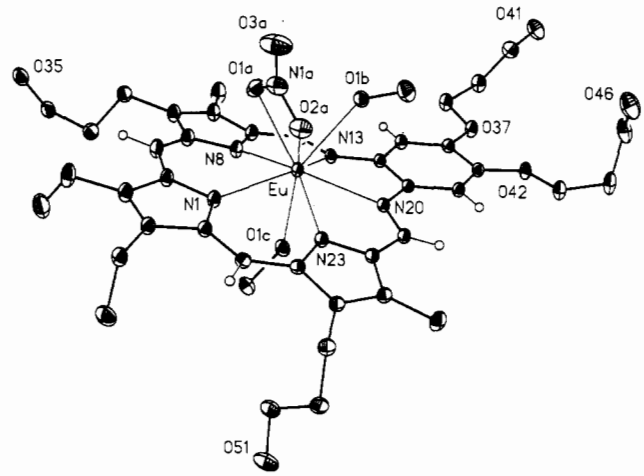

Figure 2. View of europium(III) texaphyrin **36** with the heteroatoms labeled. The analogous Gd(III) complex, **37**,[18] is isomorphous and is not shown. Most hydrogen atoms are omitted for clarity. Thermal ellipsoids were scaled to the 30% probability level. See Table II for the pertinent geometric parameters.

coordination chemistry and expanded porphyrin metal chelation. These are discussed more fully in the paragraphs below.

In the La(III) complex **3** (Figure 1), the metal cation is 10-coordinate, being ligated by two bidentate nitrate counterions (top) along with one molecule of methanol (bottom). Here, in this 1:1 metal to ligand complex, the La(III) cation is displaced from the N5 plane by 0.914 Å. The crystal structures of the Eu(III) complex **36** and the Gd(III) complex **37** were found to be isomorphous (see Figure 2). In both cases, the nine-coordinate metal cations were found to lie approximately 0.6 Å from the macrocyclic N5 plane. In addition, each complex contained one bidentate nitrate counterion and two molecules of methanol (top and bottom). In the case of the second Gd(III) complex **9**, two distinct structures were found in the unit cell (see Figure 3). In the first structure, the geometry of the nine-coordinated Gd(III) cation resembles complex **37**, being ligated by one bidentate nitrate counterion and two methanol molecules. In the second structure the Gd(III) cation was found to be 10-coordinate, being surrounded by two bidentate nitrate counterions and one molecule of methanol. Thus, this latter structure bears greater similarity to the La(III) complex **3** discussed above than to the isomorphous, nine-coordinate Eu(III) and Gd(III) complexes **36** and **37**.

In the case of the Lu(III) complex **22**, the Lu(III) cation was found to be eight-coordinate (Figure 4). It is ligated by a single bidentate nitrate and one molecule of methanol. The Lu(III) cation lies slightly above the plane of the macrocycle being displaced by approximately 0.27 Å from the mean plane of the five nitrogens. This texaphyrin structure thus stands in marked contrast to that of a five coordinate, η^4 lutetium(III) octaethylporphyrin complex. In this latter complex, the metal was found to lie approximately 0.92 Å above the macrocyclic plane.[6f] This difference in "nearly in plane" versus "essentially out of plane" binding is considered to be a direct reflection of the expanded nature of texaphyrin binding core; it has been estimated previously to be approximately 20% larger than that of the corresponding tetradentate porphyrins.[16]

This conclusion of better size matching for the texaphyrins is also apparent by inspection of the other Ln(III) texaphyrin

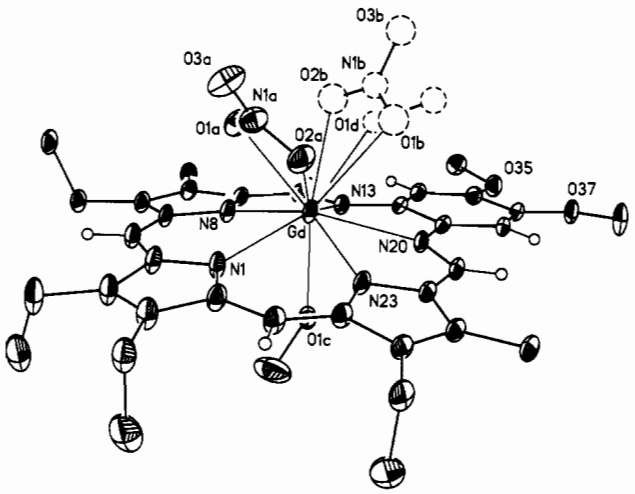

Figure 3. View of complex **9** showing the 9- and 10-coordinate Gd(III) species present in the solid state. The disordered atoms are represented as dashed circles. The half-occupancy bidentate NO_3^- ion (N1B) has considerably longer O–Gd contacts than the full occupancy NO_3^- ion (N1A): Gd–O1A, O2A 2.514(3) Å (average); Gd–O1B, O2B 2.687(7) Å (average). The disordered CH_3OH contact, O1D, is quite short (2.363-(6) Å). See Table II for other pertinent geometric parameters. Thermal ellipsoids are scaled to the 30% probability level and all heteroatoms are labeled. Most hydrogen atoms are omitted for clarity.

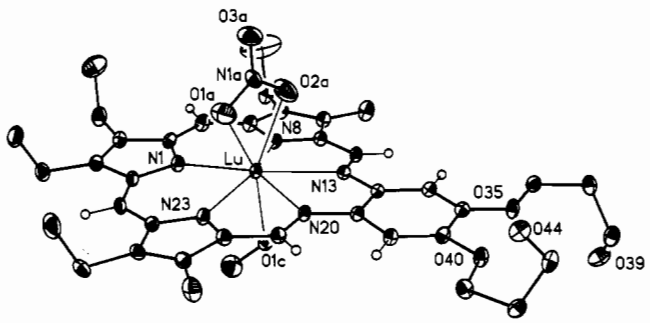

Figure 4. View of complex **22** with the heteroatoms labeled. Thermal ellipsoids are scaled to the 30% probability level, and most hydrogen atoms are omitted for clarity. The methanol coordination is shown. The 8-coordinate Lu(III) has a nearly linear O–Lu–N (NO_3^-) angle (174.1-(1)°). Other pertinent geometric details are listed in Table II.

structures discussed above (namely those of **3**, **9**, **36**, and **37**). In these cases, the Ln(III) to N5 plane distance range between 0.60 and 0.91 Å. This is significantly shorter than the metal to porphyrin mean N4 plane distances found in corresponding lanthanide porphyrin structures.[6b-h] Indeed it is to be noted that, the increased binding core of the pentadentate texaphyrin macrocycle accommodates the Ln(III) cations in a 1:1 fashion. This is in marked contrast to europium(III) and cerium(III) octaethylporphyrin complexes which have been structurally characterized as 2:1 "sandwich" or 3:2 "triple decker sandwich" with N4-metal distances on the order of 1.4 Å and 1.4 and 1.9 Å, respectively.[6b-h]

In all the above solid-state structures, a certain degree of buckling in the macrocyclic framework was observed, which depended on the size of the lanthanide cation involved. In general, the larger the Ln(III) cation the greater degree of buckling. These trends, which were entirely expected, reflect similar findings in the case of non-lanthanide porphyrins.[34] For instance, the maximum deviation from planarity (as reflected in the mean deviation of the 27 non-hydrogen atoms of the macrocyclic framework) is 0.15 Å for the La(III) complex **3** but only 0.072 for the smaller Lu(III) analogue **22**. In addition, the above structures all exhibited methanol coordination from the bottom of the metal center. Once again, the distance of the methanol

(34) See, for instance, Hoard, J. L. in *Porphyrins and Metalloporphyrins*, Smith, K. M., Ed.; Elsevier: Amsterdam, 1975, Chapter 8.

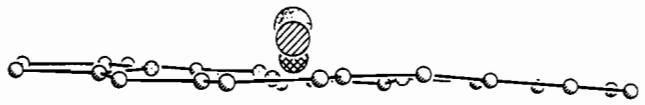

Figure 5. Schematic "overlay" representation of complexes **3**, **37**, and **22** illustrating the variation in distance above the N_5 plane of the La(III) (dotted circle, 0.91 Å), Gd(III) (lined circle, 0.60 Å) and Lu(III) (cross-hatched circle, 0.27 Å). The Ln(III) ions were oriented by best fitting (i.e., superimposing) the nitrogen donor atoms of the macrocycles by least-squares methods. The conformation of the macrocycle shown is that for lutetium(III) texaphyrin (**22**). The cation spheres are scaled to one-fourth of the ionic radii given in Shannon[42] for 10-, 9-, and 8-coordinate La^{3+} (1.27 Å), Gd^{3+} (1.11 Å), and Lu^{3+} (0.98 Å), respectively.

Table II. Selected Bond Lengths (Å) and Angles (deg) for Lanthanide(III) Texaphyrin Complexes[a]

	3	**9**	**22**	**36**	**37**
N1	2.615(4)	2.517(4)	2.421(4)	2.500(2)	2.494(4)
N8	2.506(5)	2.401(5)	2.312(4)	2.388(3)	2.383(4)
N13	2.631(5)	2.564(5)	2.455(4)	2.538(2)	2.536(3)
N20	2.685(3)	2.579(4)	2.428(3)	2.517(2)	2.517(4)
N23	2.484(5)	2.407(5)	2.324(4)	2.395(2)	2.388(4)
O1A	2.640(3)	2.508(4)	2.378(5)	2.495(2)	2.489(4)
O2A	2.642(3)	2.521(4)	2.373(4)	2.499(2)	2.484(3)
O1B	2.749(4)	2.68(1)			
O2B	2.678(3)	2.694(9)			
O1C	2.722(3)	2.512(3)	2.269(3)	2.491(2)	2.491(4)
$\Delta(N_5)^b$	0.914	0.694	0.269	0.606	0.595
C6,C27[c]	130.7(4)	130.2(4)	129.2(3)	129.7(2)	130.0(3)
C12,C21[c]	119.0(4)	118.2(3)	117.9(3)	117.4(2)	117.8(2)
N13,N20[c]	124.0(3)	123.2(3)	123.2(2)	124.0(1)	124.2(2)
N_p[d]	72.8(1)	75.4(1)	77.5(1)	75.08(6)	75.6(1)
$N_{p,i}$[d]	63.52(9)	65.5(1)	68.55(9)	66.34(5)	66.41(9)
N_i[d]	60.8(1)	62.0(2)	65.4(1)	63.53(7)	63.7(1)
NO_3^-[e]	117.2(3)	115.2(4)	114.9(4)	116.5(3)	116.2(5)
O–Ln–O[e]	47.6(1)	50.7(2)	51.9(2)	51.16(8)	51.52(13)
O1C–Ln–N_5[f]	86.7	87.5	85.4	87.5	87.1
N1A–Ln–N_5[f]	56.7	43.9	88.1	64.9	64.8
N1B–Ln–N_5[f]	47.4	55.6			
O1B–Ln–N_5[f]		49.2		50.6	50.8

[a] Unless otherwise noted, the distances (Å) given are for the separation between the indicated atom and the trivalent lanthanide cation. In all cases the atom labeling scheme is the same as that given in Figure 1. [b] The distance (Å) to the lanthanide(III) cation from the mean plane through the five-coordinating nitrogen atoms of the macrocycle. [c] Refers to the average internal angle about this atom and its next-adjacent atom within the ring; i.e., C6,C27 denotes the average angle about these two meso-like methine carbons, namely C7–C6–C5 and C2–C27–C24, respectively. [d] N_p refers to the average N–Ln–N angle involving adjacent pyrrole nitrogens, i.e., N1–Ln–N8; $N_{p,i}$ refers to the average N–Ln–N angle involving a pyrrole nitrogen and that of its adjacent imine; N_i is the N–Ln–N angle defined by the two imine nitrogens. [e] Values are the "bite" angle, O1A–N1A–O2A, on the coordinated NO_3^- ion. The values listed for O–Ln–O refer to the angle at the Ln of the coordinating oxygen atoms of a bidentate NO_3^- ion. The values for **9** do not include the half-occupancy coordinated NO_3^- ion. Those for **3** are averages. [f] The values given are the angles between the line connecting the listed atoms and the plane through the five-coordinating nitrogens of the macrocycle.

oxygen to Ln(III) cation depended on size. The La–O_{MeOH} distance, 2.722(3) Å, was slightly elongated compared to that of the Eu(III) complex **36** (2.491(2) Å), the Gd(III) analogues **9** and **37** (2.512(3) and 2.491(4) Å, respectively), or the Lu(III) congener **22** (2.269(3) Å).

In spite of the above complexities, it is clear from X-ray analysis that the Ln(III) cations (i.e., La, Eu, Gd, Lu) are coordinated to all five of the nitrogen atoms within the macrocycle and that these materials are in fact bona fide 1:1 complexes in the solid state. Because of this, they provide a unique opportunity for the study of lanthanide coordination chemistry. In particular, they allow an assessment of the intrinsic contraction of the lanthanide-(III) series as it relates to a basic pentagonal planar coordination environment. As shown in Figure 5, which provides an overlay of La(III) complex **3**, the Gd(III) complex **37**, and the Lu(III) complex **22**, this contraction serves to reduce the extent of which

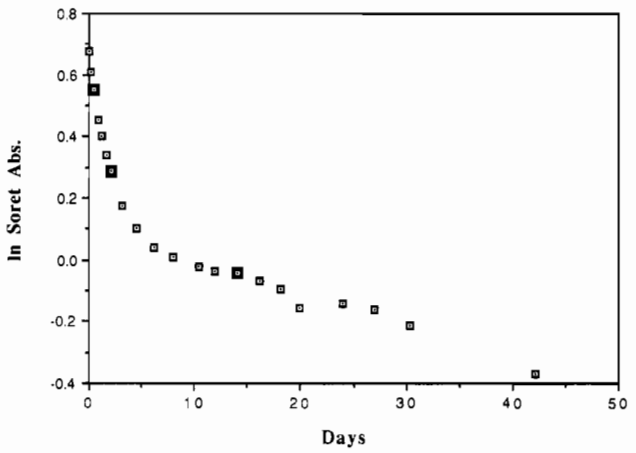

Figure 6. Natural log plot of the change in absorption at 469 nm as a function of time for complex **37** in the presence of 0.05 M EDTA at pH 7. The concentration of the starting complex is ca. 1×10^{-5} M.

the metal center is held above the mean N5 plane. It also serves, as the series is transversed, to reduce the total coordination from 10 to 8. Thus, it is important to appreciate that some, if not all, of the "into plane migration" of the metal center demonstrated by Figure 5 could be a reflection of the fact that the dissymmetry of the apical ligation is lower, for instance, in the case of the lutetium complex, than the lanthanum complex (so that the metal is not pulled up, out of the N5 plane by quite so much). Indeed, a comparison between the present lanthanide(III) complexes and the earlier-reported cadmium(II) analogues,[16b] where both in and out of plane metal binding was observed depending on the symmetry or nonsymmetry of the apical ligation, leads us to predict that complete in-plane binding could be observed for those cations, such as gadolinium(III), that are nearly the same size as cadmium(II) *provided an appropriate symmetric apical ligation geometry could be provided.* Be that as it may, it is nonetheless clear that the basic features of lanthanide coordination chemistry, namely ionic radius decrease and coordination number reduction, are reflected well in the texaphyrin series. Thus, the present results serve to support the generalized conclusions made in the context of earlier-studied but structurally unrelated neutral hexadentate Schiff-base systems.[5]

Kinetic Stability Studies. To determine the relative kinetic stability of the water soluble Gd(III) complex **37** in aqueous media, tests were carried out in the presence of three challengers: ethylenediaminetetraacetic acid (EDTA) and two anions, oxalate and phosphate. EDTA forms strong complexes with gadolinium(III) (log K = 16.7–17.4)[12e] while oxalate and phosphate form insoluble precipitates with free gadolinium(III).

For this series of tests, 50 mM stock solutions of EDTA and sodium oxalate were prepared. In addition, a 10 mM phosphate buffer was also prepared. Each of these solutions was adjusted to pH 7. Approximately 10^{-5} M of **37** was then dissolved into each of the challenger-containing test solutions. The absorbance of the resulting solutions was monitored by UV/vis spectroscopy for 45 days. Initially, a rapid decrease in the λ_{max} peak heights (but not integrated oscillator intensity) of the Soret and Q-type bands was observed (for the first 5 days) followed by a much slower decrease in the absorbance of these bands over the next 40 days. No appreciable shift in the position of the Soret or Q-type band was noticed over this time. However, broadening of the bands was observed.

A plot of the natural log of the absorbance of the Soret-type band versus time is shown in Figure 6 for the complex in EDTA solution. Similar plots were obtained from the other two test solutions. The data indicate that two separate first-order decay processes, corresponding possibly to two different first order or pseudo-first-order reactions, are occurring in each test solution. By treatment of the data for the fast component separately from the slower component, the rate constant and half-life for the faster and slower processes in each test solution could be calculated, respectively. The results are summarized in Table III.

Table III. Dynamics of Soret Band Decay for the Gadolinium(III) Texaphyrin Complex **37** Determined in the Presence of Various Putative Competing Chelating Agents[a]

	fast rate		slow rate	
	k_f, day^{-1}	$t_{1/2}$, day	k_s, day^{-1}	$t_{1/2}$, day
EDTA[b]	1.3×10^{-1}	5.5	1.1×10^{-2}	65.4
oxalate[b]	4.9×10^{-2}	14.2	1.2×10^{-2}	59.6
phosphate[c]	5.7×10^{-2}	12.3	9.1×10^{-3}	76.3

[a] Rates were determined by treating the change in absorbance at 469 nm as a function of time as the sum of two different exponentials. k_f and k_s thus refer to the resulting fast and slow exponential components, respectively. In all cases, the initial concentration of complex **37** was 1×10^{-5} M and the initial pH = 7. [b] The starting EDTA (ethylenediaminetetracetic acid) and sodium oxalate concentrations were 0.05 M. The pH of the former solution was adjusted to pH 7 by the careful addition of NaOH. [c] The term "phosphate" refers to 0.01 M pH 7 phosphate buffer.

High complex stability is a known prerequisite for MRI applications.[11] Thus it was important to determine what these fast and slow decay components (i.e., k_f and k_s in Table III) represent in terms of actual kinetic stability. In particular, we were concerned lest the fast decay reflected a rapid demetallation that, presumably, would give rise to *toxic* $Gd(III)(H_2O)_6^{3+}$ and the free-base form of the texaphyrin. This latter material, it was thought, could then, in turn (as the slow decay process), undergo further hydrolysis and/or decomposition into its constituent nonabsorbing components.

To test the above possibility, a concentrated solution of **37** was incubated in a 0.1 M aqueous solution of EDTA (pH = 7.3) at room temperature in the dark for 1 week. Here again, the absorbance of the complex in this solution was monitored periodically by UV/vis spectroscopy. No shift in the position of the Soret and Q-type bands was observed. Only a decrease in the intensity of these bands was observed, just as in the initial experiment. After 1 week, the green colored material remaining was isolated and subjected to FAB mass spectrometric analysis. The results revealed a peak corresponding to the metal complex **37** only, with no peak for the free-base macrocycle being present.[35] This indicates that the fast reaction does not correspond to rapid demetalation of the complex with concomitant formation of the free-base macrocycle.

The above finding leads us to suggest that the observable species in solution, over the entire 45-day period, is the gadolinium(III) texaphyrin complex. This conclusion is further supported by the lack of any observable shifts in the position of the Soret and Q-type bands over the 45-day period: If appreciable amounts of free-base macrocycle were being formed, a shift in the position of these bands would be expected.[36] These results indicate that the Gd(III) complex **37** is stable *in vitro* in the presence of strong chelating agents, such as EDTA, at pH 7 for a long period of time. It also means that this complex may possess sufficient stability to allow its use as a paramagnetic contrast agent *in vivo*. The stability of **37** is in marked contrast to the Gd(III) porphyrins, which are known to demetallate rapidly in the presence of EDTA.[6j,l,m]

The above conclusion with regards to hydrolytic nonlability, although clearly central to this work, does not explain the observed absorption dynamics. Thus, a new hypothesis for the fast reaction was proposed. This hypothesis entails aggregation. Water soluble porphyrins are known to aggregate in aqueous solution and it was considered likely that **37** would behave similarly.[37] This assesment

(35) The free-base form of the texaphyrin macrocycle is detected by FAB MS under these experimental conditions; see ref 16b.
(36) The optical spectrum of the free-base texaphyrin has been identified, the Q-type band of the free-base is shifted by ca. 10–15 nm to the blue relative to metal complexes; see ref 16b.
(37) White, W. I. in *The Porphyrins*; Dolphin, D. Ed.; Academic: New York, 1978–1979; Vol. V, Chapter 7.

is consistent with the fact that the λ_{max} peak heights but not integrated oscillator intensity are observed to decrease as a function of time.

Several experiments were performed to test further the above hypothesis. First, using EDTA as the challenger, the optical behavior of aqueous solutions of **37** was observed as a function of varying concentrations of EDTA. In this series of experiments, the concentration of **37** was held constant (ca. 10^{-5} M) while the concentration of EDTA was varied from 0.1 M to 0.001 M (at pH 7.3). The rate of the fast presumed reaction was found to be roughly the same in all concentrations of EDTA used. This indicates the fast reaction is not dependent on the concentration of EDTA. In a second experiment, the concentration of EDTA was held constant (0.01 M at pH 7.3) while the concentration of **37** was varied between ca. 5×10^{-5} and 5×10^{-6} M. In this case, the rate of the fast reaction was found to be dependent on the concentration of **37**, with the rate increasing with an increasing concentration of **37**.

On the basis of the above information, the initial drop in the absorbance of the complex in the presence of EDTA is assigned as being due to the aggregation of **37** in solution. Although not subject to a similar level of qualitative analysis, similar trends were observed with the oxalate and phosphate anions. The extent of aggregation, however, cannot be determined by these simple experiments, and thus it is not known if it is dimers, trimers, or higher oligomers that are being formed as a result of this fast reaction. Such a determination, however, was considered as being nonessential for the purposes of MRI enhancement testing. It was, therefore, not made in the context of the present study.

Also not made in the context of the present study were detailed kinetic analyses of the stabilities of the other lanthanide texaphyrin complexes described herein. In all cases, however, qualitative evidence was consistent with a high degree of nonlability. In other words, all complexes appeared stable for at least a few days in aqueous solution under ambient laboratory conditions. In the case of the lanthanum(III) complex **31**, however, prolonged exposure to water, especially at low pH and/or in the presence of light, led to evident decomposition. This decomposition, which was not observed in the case of the other complexes (at least on any reasonable time scale), was accompanied by the concomitant production of red, presumably polypyrrolic, pigments.

Relaxivity Properties. From the X-ray crystal structure of the water soluble Gd(III) texaphyrin **37**, we discern that this complex should have at least four open coordination sites for the binding water. Therefore, Young and co-workers[18,38] measured the relaxivity of the Gd(III) complex **37**. In aqueous solution at 25 °C, the longitudinal relaxivity, R_1, of **37** was found to be 19.0 ± 1.5 mM^{-1} s^{-1} at 20 MHz. This relaxivity was also independently measured by Geraldes and Sherry.[39] These workers found the R_1 relaxivity of **37** to be 16.9 ± 1.5 mM^{-1} s^{-1} at 50 MHz. in aqueous solution and found it to be invariant in magnitude over a period of 4 days (in fact, it increased slightly). This observed invariance in R_1 thus serves to underscore further the high kinetic stability of **37** in aqueous media. Geraldes and Sherry also determined the relaxivity of **37** in 0.01 M phosphate buffer (pH ~ 7) at 50 MHz and 20 °C. Under these conditions, the relaxivity of complex **37** was significantly lower, being 5.3 ± 0.7 mM^{-1} s^{-1}.[39] This observed lower R_1 may simply reflect that the Gd(III) complex **37**, as do other Ln(III) complexes, binds strongly to phosphate.[10a] Such a binding would hinder the accessibility of bulk water to the Gd(III) center and reduce the relaxivity of the complex. These points, however, will be discussed more fully in a separate report.[39]

Table IV compares the R_1 relaxivity of **37** in aqueous solution with the relaxivities of $[Gd^{III}DTPA]^{2-}$, $[Gd^{III}DOTA]^{-}$, $[Gd^{III}$HP-DO3A], and the Gd(III) aquo ion, $[Gd(H_2O)_8]^{3+}$. It is noteworthy that **37** has a higher relaxivity than the aquo ion of Gd(III). This same phenomenon has been observed in the case of water soluble porphyrins.[6,40] Thus, based on the relaxation of inner sphere water alone, one would expect that the aquo ion of Gd(III) should possess a higher relaxivity. However, this is not the case. This then seems to indicate that there are other mechanisms, including possibly various spin–orbit interactions, that are contributing to the high observed relaxivities.[11] In any case, the high R_1 of **37** stands as important augury for its effective use in MRI contrast applications.

Table IV. Longitudinal Relaxivity Values (R_1) for Various Water Soluble Gadolinium(III) Complexes[a]

complex	R_1, mM^{-1} s^{-1}	freq, MHz	temp, °C	ref
37	19.0	20	25	18, 38
37	16.9	50	25	39
$[GdDTPA]^{2-}$	3.7	20	37	11a
	4.5	20	37	5d, 11a
$[GdDOTA]^{-}$	3.4	20	37	11a,b
[GdHP-DO3A]	3.6	20	40	14g–i
$[Gd(H_2O)_8]^{3+}$	9.1	20	35	11a

[a] DTPA = diethylentriaminepentaacetic acid pentaanion; DOTA = 1,4,7,10-tetraazacyclododecane-*N*,*N*′,*N*″,*N*‴-1,4,7,10-tetraacetic acid tetraanion; HP-DO3A = 10-(2-hydroxypropyl)-1,4,7,10-tetraazacyclododecane-*N*,*N*′,*N*″,*N*‴-1,4,7-triacetic acid trianion.

Summary and Conclusion

The present work has shown a novel approach to forming water soluble 1:1 lanthanide(III) complexes. In the case of the Gd(III) chelate **37**, the lack of lability under model physiological conditions and the high observed longitudinal relaxivity in aqueous solution has led us to suggest that this material, or other gadolinium(III) texaphyrin complexes, could be used in a variety of MRI-type enhancement applications.[38] Current work, some of which is reported elsewhere,[18] is focused on testing further[38] the experimental merits of this possibility.

Acknowledgment. This work was supported by grants from the NIH (AI 28845), NSF (CHE 9122161), the Camille and Henry Dreyfus Foundation (Teacher-Scholar Award to J.L.S., 1988–1992), and Pharmacyclics Inc. T.D.M. wishes to thank the UT Austin Department of Chemistry for a Texaco Foundation Fellowship (1991–1992). We are grateful to Miguel Rosingana, Roberto Espinoza, and George Churchill for synthetic assistance. We wish to thank Professors Stuart Young and A. Dean Sherry and Dr. Carlos F. G. C. Geraldes for help with MRI relaxivity measurements. We wish to thank Professor Young for making available the results of *in vivo* studies prior to publication.

Supplementary Material Available: Five appendices, each containing tables of atomic thermal factors, atomic positional parameters, and bond distances and angles for texaphyrin structures, and supplementary figure(s), showing atom labeling schemes, for lanthanide(III) texaphyrin structures **3**, **36**, **37**, **9**, and **22** (65 pages). Ordering information is given on any current masthead page.

(38) Sidhu, M. K.; Muller, H.; Miller, R. A.; Mody, T. D.; Hemmi, G.; Sessler, J. L.; Young, S. W. *Abstr. 1991 Natl. Mtg. Am. Assoc. Univ. Radiol.* **1991**. See also, ref 18.

(39) Geraldes, C. F. G. C.; Sherry, A. D. To be published.

(40) For examples of MRI studies using porphyrins, see: (a) Mosseri, S.; Mialocq, J. C.; Perly, B.; Hambright, P. *J. Phys. Chem.* **1991**, *95*, 4659–4663 and references therein. (b) Bohdiewicz, P. J.; Lavallee, D. K.; Fawwaz, R. A.; Newhouse, J. H.; Oluwole, S. F.; Alderson, P. O. *Invest. Radiol.* **1990**, *25*, 765–770 and references therein. (c) Furmanski, P.; Longley, C. *Cancer Res.* **1988**, *48*, 4604–4610. (d) Patronas, N. J.; Cohen, J. S.; Knop, R. H.; Dwyer, A. J.; Colcher, D.; Lundy, J.; Mornex, F.; Hambright, P.; Sohn, M.; Myers, C. E. *Cancer Treat. Rep.* **1986**, *70*, 391–395. (e) Jackon, L. S.; Nelson, J. A.; Case, T. A.; Burnham, B. F. *Invest. Radiol.* **1985**, *20*, 226–229. Also, see ref 6 above.

(41) Many porphyrins are also known to be retained selectively by neoplastic tissues. See, for instance, refs 6 and 40.

(42) Shannon, R. D. *Acta Crystallogr.* **1976**, *A32*, 751–767.